

PACWAVE WAVE RESOURCE ASSESSMENT

Prepared by:

Gabrielle Dunkle, Oregon State University

Bryson Robertson, Oregon State University*

Gabriel García-Medina, Pacific Northwest National Laboratory

Zhaoqing Yang, Pacific Northwest National Laboratory

*bryson.robertson@oregonstate.edu



TABLE OF CONTENTS

1 Introduction.....2

2 Newport Buoys and SWAN Hindcast Model2

3 Wave Resource Characteristic Parameters.....4

4 Wave Resource Results6

 4.1 Annual histogram of sea state occurrences.....6

 4.2 Annual wave rose7

 4.3 Annual variation of long-term monthly mean8

 4.4 Monthly cumulative distributions17

5 Temporal Fluctuation of IEC Parameters.....22

6 Wind Effect at PacWave.....24

7 Extreme Environmental Contours29

8 Operation & Maintenance Windows32

9 Conclusions.....39

7 References.....41

Appendix A: PacWave North Wave Results.....42

 A.1 Annual histogram of sea state occurrences42

 A.2 Annual wave rose.....43

 A.3 Annual variation of long-term monthly mean.....44

 A.4 Monthly cumulative distributions47

 A.6 Extreme Environmental Contours51

 A.7 Operation & Maintenance Windows52



Note: Document has been updated (Nov. 2020) to reflect wave energy resource at centroid of PacWave South test site and northeast corner of PacWave North test site. The previous edition described wave energy at a location ~1 mile east of PWS centroid. New results prove the resource has not changed significantly between the two locations, and all conclusions from the previous edition still stand.

1 INTRODUCTION

The Pacific Northwest of the United States is characterized by one of the greatest annual mean wave power resources in the world [1]. As a result, the wave energy resource offshore of Oregon has been characterized, through hindcast models and physical buoy data, throughout the past decade [2]–[4]. Over the past 8 years, Oregon State University (OSU) has been developing an open-ocean wave energy test facility, PacWave, which is affiliated with the Pacific Marine Energy Center (PMEC). The facility consists of north and south test sites off the coast of Newport, Oregon.

This report contains detailed analysis of wave characteristics at both the north and south sites based on a newly available 32-year SWAN hindcast simulation [5] and follows the recommendations issued by the International Electrotechnical Commission (IEC) technical specification (TS) 62600-101 for wave energy resource assessments [6]. This assessment aims to build upon the previous wave energy characterizations in the region and provide the most up-to-date characterization of the wave energy resource at PacWave.

2 NEWPORT BUOYS AND SWAN HINDCAST MODEL

There are various sources for physically observed sea state data in the PacWave region. PMEC measured meteorological, wind, wave, current, and ocean surface salinity and temperature data at PacWave South from November 2014 through January 2015, and again from May 2015 through December 2015. Additionally, the Ocean Observatories Initiative of the National Science Foundation has collected physical wave data spanning from January 2015 through April 2019; located at 44°38'21"N 124°18'15"W and 80 m depth. In the general vicinity are multiple National Oceanographic and Atmospheric Administration (NOAA) National Data Buoy Center (NDBC) stations as well, from which various data are highlighted in this report.

The specific location of the model for the purpose of this assessment is the PacWave North site at 44.7021°N, 124.146°W and the PacWave South site at 44.557°N, 124.229°W, which are about 10 miles (16 km) apart and off the coast of Newport, Oregon, demonstrated in Figure 1. The point chosen for PacWave North is 0.3 miles north of the northeast corner of the test site while the point for PacWave South is almost in the exact center of the site. The mean depth at the PacWave North point is 53.0 m and 67.4 m for PacWave South. PacWave South results are examined in the main text of this report; corresponding PacWave North results can be found in the Appendix.

This wave resource assessment was conducted from the years 1980-2010, part of a 32-year hindcast conducted by the Pacific Northwest National Laboratory (PNNL) [5], which operates within the U.S. Department of Energy. The hindcast model constructed by PNNL used nested-grid WaveWatch III (WW3) wave model on both global and regional scales [5]. The WW3 model was paired with a high-resolution, unstructured-grid Simulating WAVes Nearshore (SWAN) model via traditional one-way nesting. Both models are forced by Climate Forecast System Reanalysis (CFSR) wind fields [5]. These models are classified as in between a Class 1 Reconnaissance study and a Class 2 Feasibility study by the IEC standard due to their temporal and spatial resolutions [4][5], therefore this IEC specification assessment can generally be classified as a Class 1 Reconnaissance study [6].

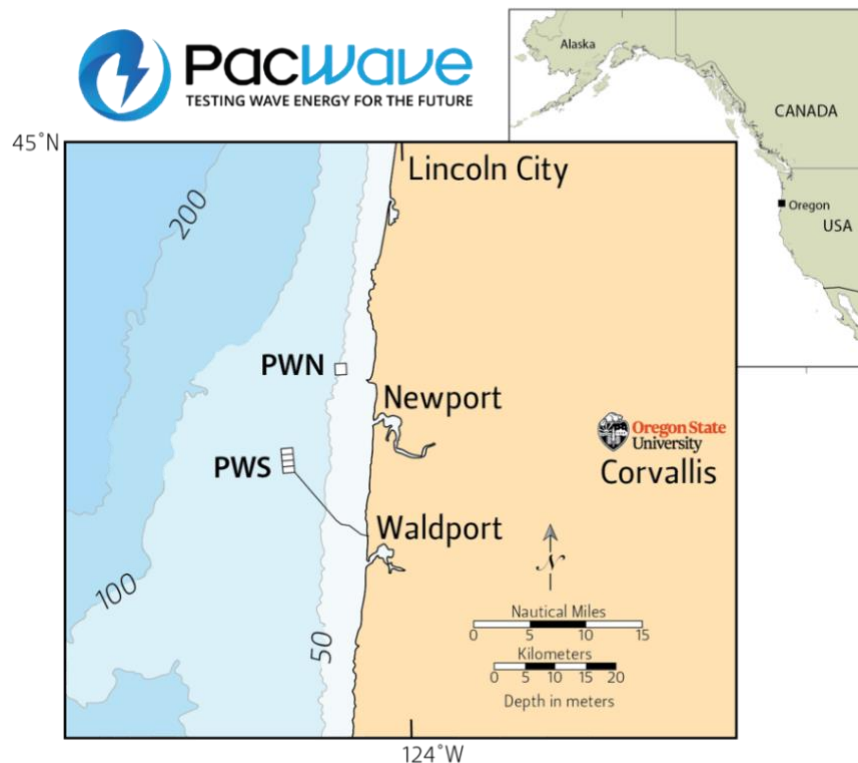


Figure 1: PacWave North (PWN) and South (PWS) locations off the coast of central Oregon (PacWave, 2020)

The use of SWAN with CFSR winds simulates nearshore wave processes along the U.S. West Coast, and was validated by observed buoy data from 28 wave buoys in the region. Wu et al. (2020) demonstrated the congruence between the PNNL model's prediction of IEC wave energy parameters and those recorded at physical buoy stations, accurately providing a reliable wave climate model in the nearshore region of interest [5]. Satisfactory accuracy was also achieved when comparing the spectra distributions in both frequency and directional domains at sites with extreme values, i.e. regions with maximum and minimum wave energy [4]. For detailed model validation methods and results, please see Wu et al., 2020 [5].

The IEC standard states that a minimum of 10 years of data should be used for this type of assessment, however according to both the IEC specification and Yang et al. [4], a longer period of data may be necessary to quantify the low frequency climate variability and its effect on a wave energy resource assessment. This is highlighted in the wave resource results section of this assessment, where the long-term mean and its seasonal variability of each IEC wave energy resource parameters are analyzed.

3 WAVE RESOURCE CHARACTERISTIC PARAMETERS

The sea states are characterized with directional wave spectra, which are described below and sourced from the IEC TS 62600-101 [6]. The variance density described over the i^{th} discrete frequency and j^{th} discrete direction is S_{ij} .

To calculate directionally unresolved (omni-directional) characteristic quantities, the two-dimensional frequency-directional variance densities are transformed into one-dimensional frequency resolved variance densities of θ increments such that:

$$S_i = \sum_j S_{ij} \Delta\theta_j \quad (1)$$

Spectral moments of the n^{th} order, m_n , are calculated from the frequency variance density by:

$$m_n = \sum_i f_i^n S_i \Delta f_i \quad (2)$$

where f_i is the i^{th} discrete frequency. Omni-directional wave power J is the time averaged energy flux through a vertical cross section of unit diameter that extends from the seafloor to the surface, calculated by:

$$J = \rho g \sum_{i,j} c_{g,i} S_{ij} \Delta f_i \Delta\theta_j \quad (3)$$

where

$$c_{g,i} = \frac{\pi f_i}{k_i} \left(1 + \frac{2k_i h}{\sinh 2k_i h} \right) \quad (4)$$

where k_i is the wave number at the i^{th} frequency and h is the mean sea level.

The time-averaged energy flux across a plane normalized to direction θ is defined as the directionally resolved wave power. This directionally resolved wave energy transport is the sum of the contributions of each component with a positive component in direction θ , calculated by:

$$J_\theta = \rho g \sum_{i,j} c_{g,i} S_{ij} \Delta f_i \Delta\theta_j \cos(\theta - \theta_j) \delta \quad \begin{cases} \delta = 1, & \cos(\theta - \theta_j) \geq 0 \\ \delta = 0, & \cos(\theta - \theta_j) < 0 \end{cases} \quad (5)$$

The maximum value of J_θ represents the maximum time averaged wave power propagating in a single direction and is denoted by $J_{\theta Jmax}$. Angles in SWAN were calculated in Cartesian with east being the zero-degree bearing [7], and are adjusted such that North is the zero-degree bearing where necessary.

A characteristic wave height of the given sea state is calculated using the zeroth spectral moment by:

$$H_{m0} = 4\sqrt{m_0} \quad (6)$$

This is referred to as the significant wave height calculated from the wave spectrum, which is not the same value as the significant wave height calculated from a wave-by-wave analysis, $H_{1/3}$. $H_{1/3}$, commonly referred to as H_s , is a direct measure of significant wave height whereas H_{m0} is estimated based on the spectrum via (6).

The preferred characteristic wave period for wave resource assessments is the energy period. Energy period is calculated using moments of the wave spectrum by:

$$T_e \equiv T_{-10} = \frac{m_{-1}}{m_0} \quad (7)$$

The directionality coefficient is a characteristic measure of the directional spreading of wave power. It is the ratio of the maximum directionally resolved wave energy transport to the omni-directional wave energy transport:

$$d = \frac{J_{\theta Jmax}}{J} \quad (8)$$

Spectral width characterizes the relative spreading of the energy along the wave spectrum, and provides an idea of the makeup of the sea state [8]. This parameter is defined using the moments of the wave spectrum as:

$$\epsilon_0 = \sqrt{\frac{m_0 m_{-2}}{m_{-1}^2} - 1} \quad (9)$$

The preceding variables were outputs from the SWAN model used in the PNNL hindcast, whose wave parameters are computed from the wave spectrum [7]. These spectral quantities were used in the following analysis of the wave energy resource at PacWave.

4 WAVE RESOURCE RESULTS

4.1 Annual histogram of sea state occurrences

Figure 2 shows the annual frequency of occurrence of sea states parameterized in terms of the significant wave heights, H_{m0} , with a resolution of 0.5 m and energy period, T_e , with a resolution of 1 s as per the IEC specification recommendation. The numbers in each cell represent mean annual hours recorded in each specific $H_{m0} - T_e$ sea state combination. The shading of the cells is an energy flux weighted representation; with the output of particular sea state occurrence calculated by $0.5 \cdot H_{m0}^2 T_e$ multiplied by the hours of occurrence. Figure 2 shows the annual mean bivariate histogram from 1980-2010 at PacWave South.

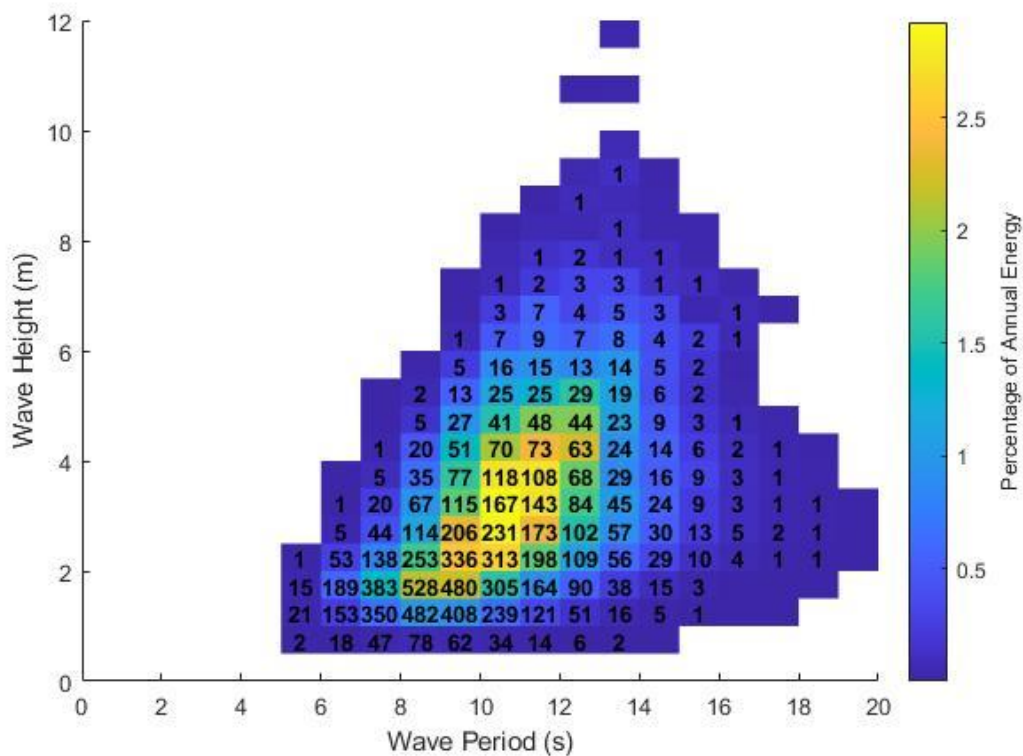


Figure 2: Omni-directional SWAN sea-state histogram from 1980-2010 at PacWave South (annual mean conditions)

At PacWave South, the most commonly occurring seas occur for 528 hours per year with a significant wave height of 1.75 m and an energy period of 8.5 s, while the highest annualized

wave energy sea state occurs for 231 hours per year at a significant wave height of 2.75 m and at an energy period of 10.5 s.

4.2 Annual wave rose

An annual wave rose depicts the long-term joint distribution of the maximum directionally resolved wave energy transport ($J_{\theta_{Jmax}}$) along the direction of maximum directionally resolved energy transport (θ_{Jmax}). Each sea state is represented by a single directionally resolved wave power and associated direction. Figure 3 shows the distributions of the total maximum directionally resolved wave energy transport in W/m. Each bar combines wave headings in a 15° bin, and the length of each color segment represents the annual wave energy transport in a given direction.

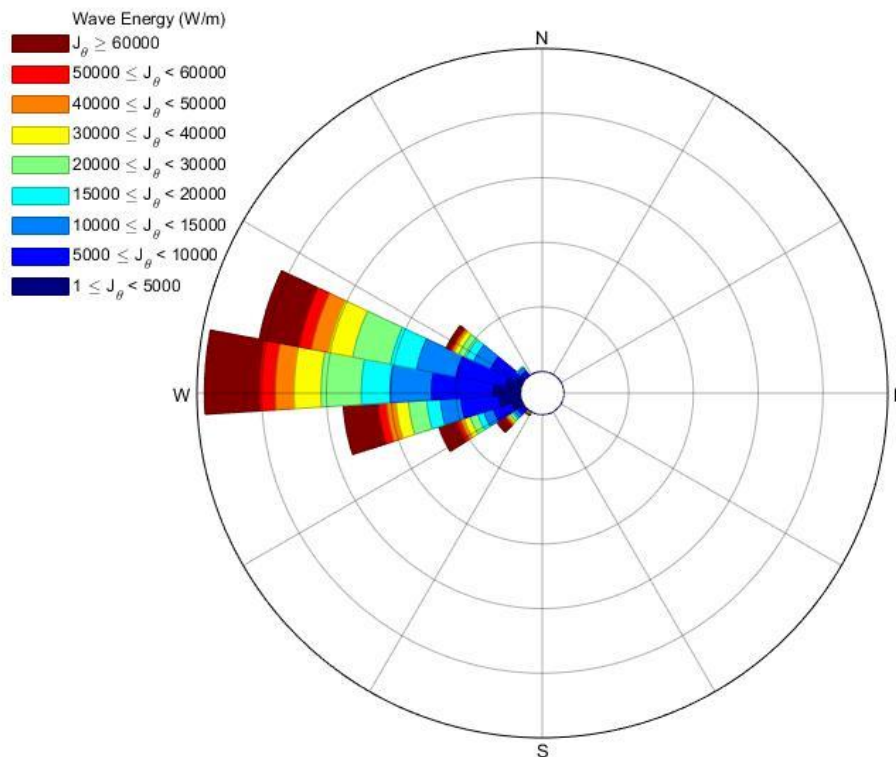


Figure 3: Directionally resolved SWAN wave rose distribution of wave energy from 1980-2010 at PacWave South

The waves come predominately from the west-northwest directions at PacWave South, accounting for the majority of the direction of directionally resolved wave energy throughout the hindcast.

4.3 Annual variation of long-term monthly mean

The long-term monthly mean of wave resource characteristic parameters required by the IEC and are analyzed in the following section. Monthly averages over the years, variations of the mean, variation of one standard deviation above and below the mean, and 10th, 50th, and 90th percentiles are plotted in order to show the statistical monthly variations. The percentile analysis is completed in order to show the limits of the datasets and identify the median. The 10th and 90th percentiles are used to show the upper and lower limits of the data, and the 50th percentile is equivalent to the median of the dataset.

In a normal distribution, the curve of a dataset is symmetric about the mean, earning the common reference of a “bell curve.” If a dataset is skewed, the shape of the distribution has asymmetric qualities. Figure 4 offers a visual perspective of skewness in a dataset by comparing variously skewed distributions. By comparing the mean and the median of the distribution, it is possible to assess the degree of skewness. If the mean value is greater than the median, the dataset is positively skewed, meaning that the distribution has the majority of occurrences on the lower end of the curve. This is typical of sea state distributions, as more extreme events are less frequent. For a detailed review of the extreme wave climate and storms on the Oregon coast, refer to Ruggiero et al. (2009) [9].

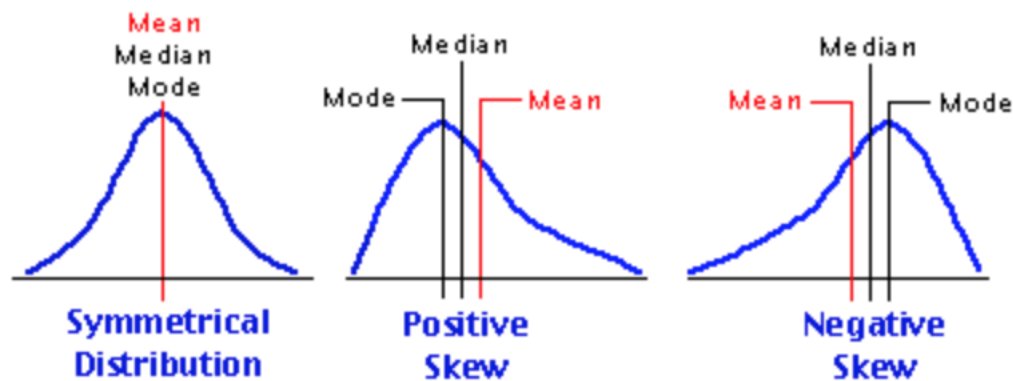


Figure 4: Skewness can be indicated by the difference of the median (50th percentile) and the mean. Larger differences between percentiles and the mean determine the degree to which the distribution is skewed. (CFA, 2020)

Figure 5 depicts the trend of significant wave height at PacWave South, demonstrating the pattern of seasonal change of the wave characteristics. The mean wave height at the site peaks in December at 3.5 m, and steadily falls to a minimum value of 1.75 m in August. In the winter, between November and March, the average wave height varies between 3 and 3.5 m, and the distribution is more positively skewed as the 90th percentile values correspond to more extreme wave height conditions. The summer months, between May and September, stay between 1.5 and 2 m, signifying a more normally distributed range of wave heights as the percentile values range closer to the mean value. This effect can be described as seasonality, where wave heights vary according to different seasons throughout year. Wave heights increase as frequency of extreme sea states increases in the winter, while summer months see smaller sea states.

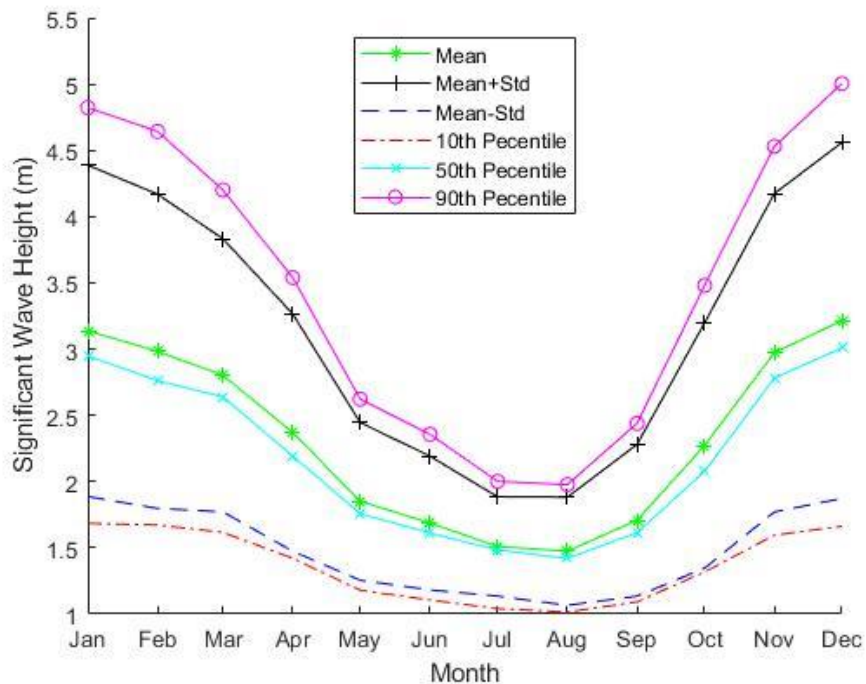


Figure 5: Monthly mean of SWAN significant wave height from 1980-2010 at PacWave South

As shown in Figure 6, the mean energy period is minimum in the summer months with values around 9 s compared to the maximum seen in winter months ranging from 11-12 s. In the summer, waves are forced primarily by local winds, inducing high frequency waves indicated by the lower wave periods. Energy period peaks in February at 11.3 s and is lowest in July at 8.5 s. Wave period is generally normally distributed, which is reflected in Figure 6.

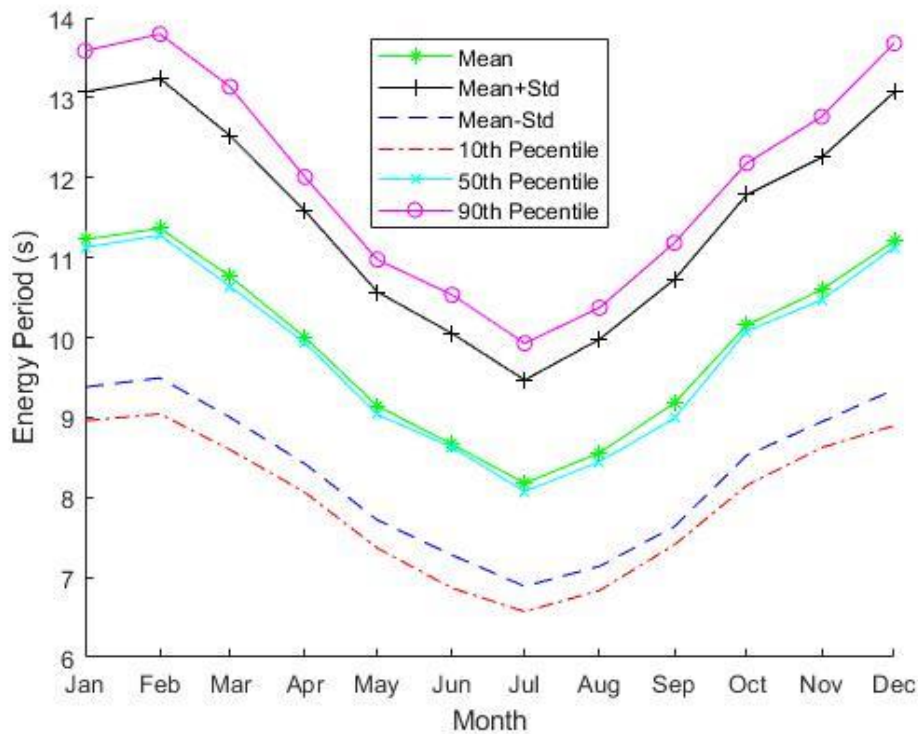


Figure 6: Monthly mean of SWAN wave energy period from 1980-2010 at PacWave South

The omni-directional wave energy transport is shown in Figure 7. The greatest average wave energy occurs in the winter months from 70-80 kW/m and stays in this range from November through February. This is expected, as winter months have more energetic seas due to storms [9]. With storms come extreme sea state events, which cause the large deviations from the mean during these months. Summer months see less variation from the mean due to less energetic sea states. This is another instance in which the data is positively skewed: the 90th percentile values are significantly larger in the winter months and stray from the mean value line, whereas summer months have percentile values that are more normally distributed about the mean.

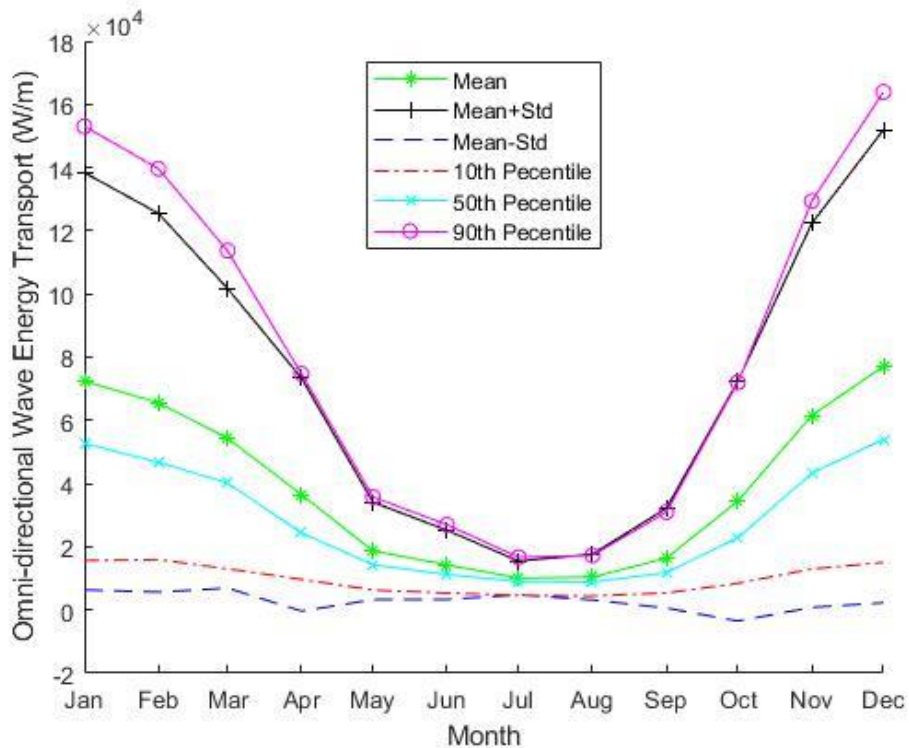


Figure 7: Monthly mean of SWAN omni-directional wave energy transport from 1980-2010 at PacWave South

Figure 8 shows the maximum directionally resolved wave energy transport. As expected, the directionally resolved wave energy transport peaks in the winter months at 75 kW/m and has a minimum in the summer at under 20 kW/m. As with the omni-directional wave energy transport, the directionally resolved wave energy transport also shows positive skewness in the winter and more normally distributed values in the summer.

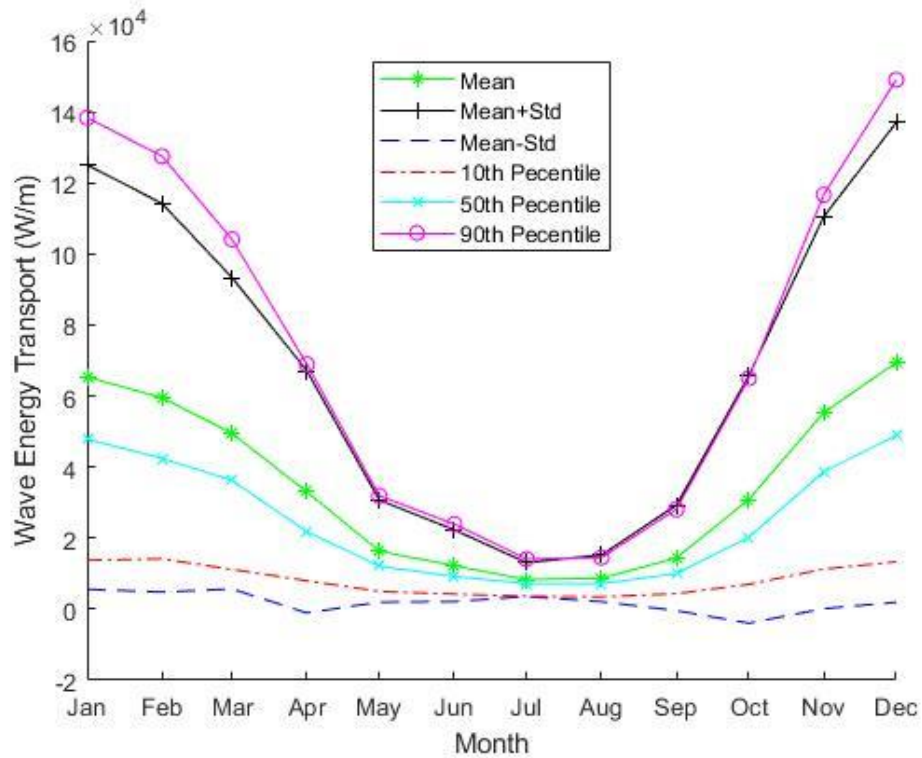


Figure 8: Monthly mean of maximum directionally resolved SWAN wave energy transport from 1980-2010 at PacWave South

Figure 9 describes the mean direction of the maximum directionally resolved wave energy transport. The direction values were adjusted such that the datum was 0° North, and all values were measured clockwise (i.e. Nautical direction convention). In doing so, all output values per 90° section of the circle were adjusted to the correct range as if they were originally measured from the 0° North datum. For example: $180 + (90^\circ - \theta)$ places measurements as though they were taken from 0° North. This method ensured that minimal wave values were recorded as if they originated from the coast and propagated offshore.

The slight variation in mean direction over time indicates that the wave field has a narrow directional change. The directional data is normally distributed about the mean, with average values ranging between 270 and 300 degrees as expected, which can be confirmed by the wave rose in Figure 3.

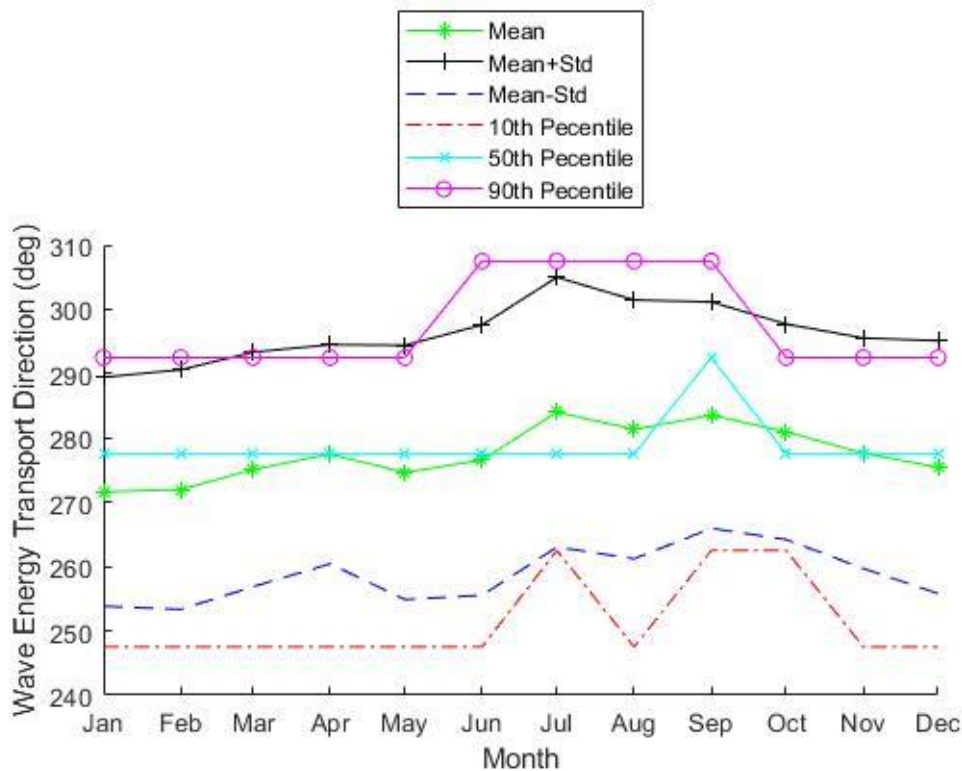


Figure 9: Monthly mean of direction of SWAN directional wave energy transport from 1980-2010 at PacWave South

Figure 10 shows that the average directionality coefficient at PacWave South varies according to season, similar to the majority of previously evaluated wave characteristics. Recall that this plot describes the ratio of J and $J_{\theta_{Jmax}}$. Higher values of directionality coefficient relate to a narrow spread of wave directions in that J and $J_{\theta_{Jmax}}$ are closer in value; approaching a value of 1 indicates that the majority of omni-directional wave energy transport is resolved to a narrow-band of directions. Since the maximum values of the directionality coefficient are seen in winter months, it can be inferred that these months see convergence to a narrower field of directions, mainly due to storm dominated sea states. In the summer, the wave field is comprised of both wind waves, that propagate in a greater variety of directions, and ocean swells. This is indicated by lower values of directionality coefficient from May through September. Overall, the mean directionality varies by less than 0.1 throughout the year, indicating a relatively constant directional bandwidth.

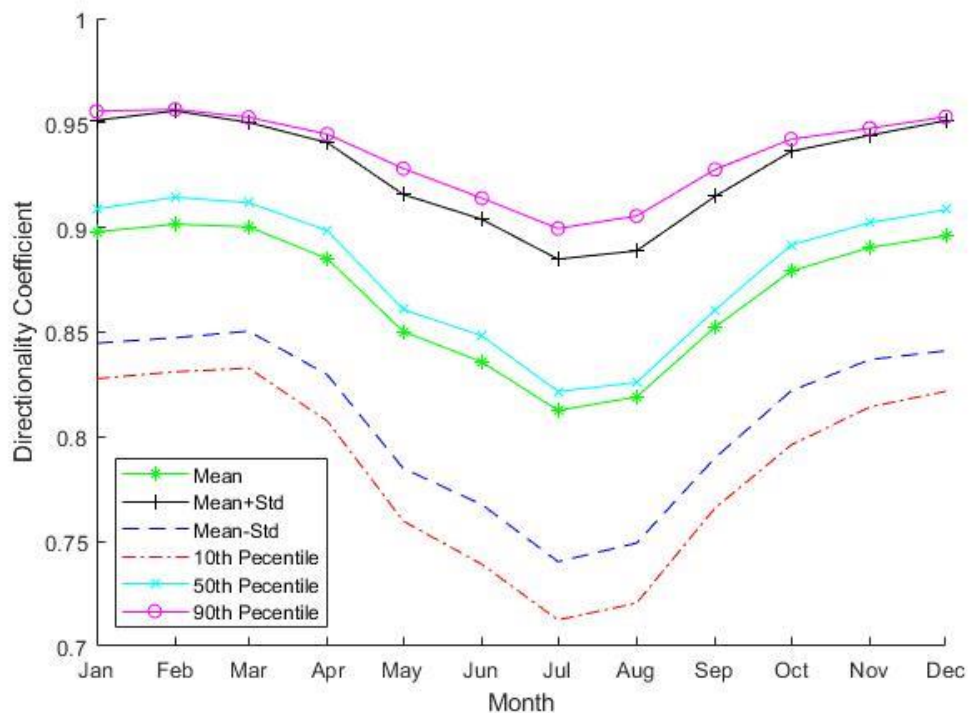


Figure 10: Monthly mean of SWAN directionality coefficient from 1980-2010 at PacWave South

When completing an IEC specification for wave energy resource, it is important to distinguish the definitions of certain attributes of a wave spectrum. Wave spreading and spectral width are similar in that they describe spreading, but these attributes can often become confused with one another. Wave spreading itself describes the directional spread of variance density in a wave energy spectrum, while spectral width describes the frequency spread of variance density. An example of wave energy spreading is shown in Figure 11, where an arbitrary spectrum's

energy is dispersed across a range of directions – which is wider than often found in nature and is purely illustrative. The directional spread of a wave energy spectrum can also be observed in wave rose figures similar to that of Figure 3, which details the main directions from which directionally resolved wave energy arrives at PacWave South. Directional bandwidth is described by directionality coefficient, as explained previously.

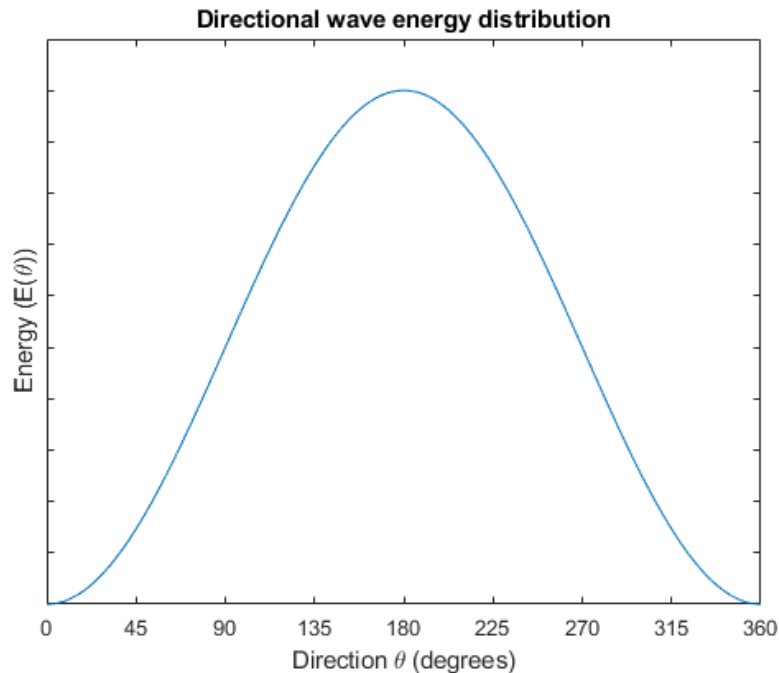


Figure 11: Spread of direction of wave energy for an arbitrary spectrum.

Spectral width is its own parameter recommended for analysis by the IEC, and it varies between 0 and 1 based on the sea state most dominant in the spectrum of interest. A swell-dominated spectrum has a spectral width value that approaches 0, in that its shape has a small width at its peak [8]. Wind-wave dominated spectra tend to have a broader range of wave conditions, with comparatively large widths at their peaks [8]. Figure 12 aims to lend a visual describing spectral width and how the parameter may vary.

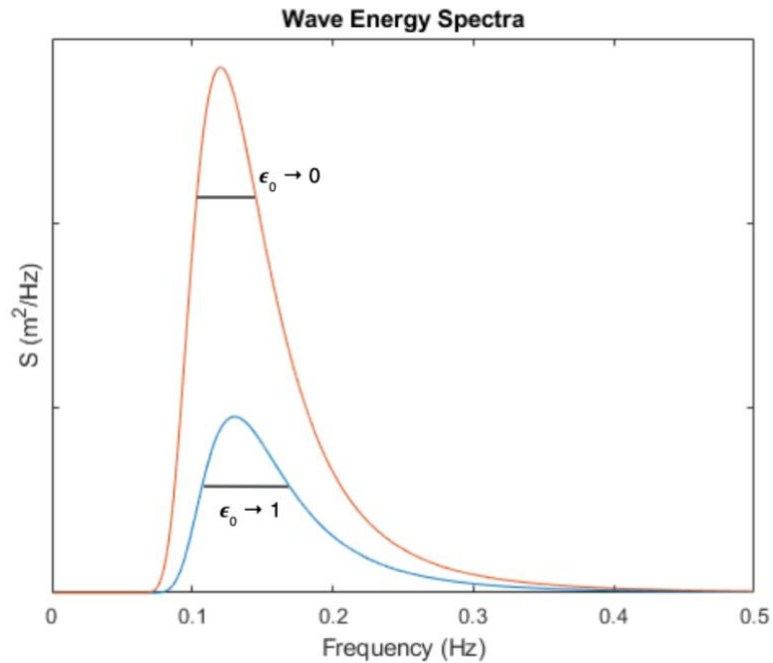


Figure 12: Comparison between two arbitrary wave energy spectra. The orange line is representative of a swell-dominated spectrum, with a spectral width approaching 0. The blue line represents a wind-wave dominated spectrum where its spectral width goes to 1.

The average spectral width over the hindcast at PacWave South is shown in Figure 13. Low spectral width values in the winter months are due to a swell dominated energy spectrum, where the parameter is expected to go to 0. Spectral width increases and goes toward a value of 1 as the wave field variation increases in the summer months, when waves are primarily wind driven.

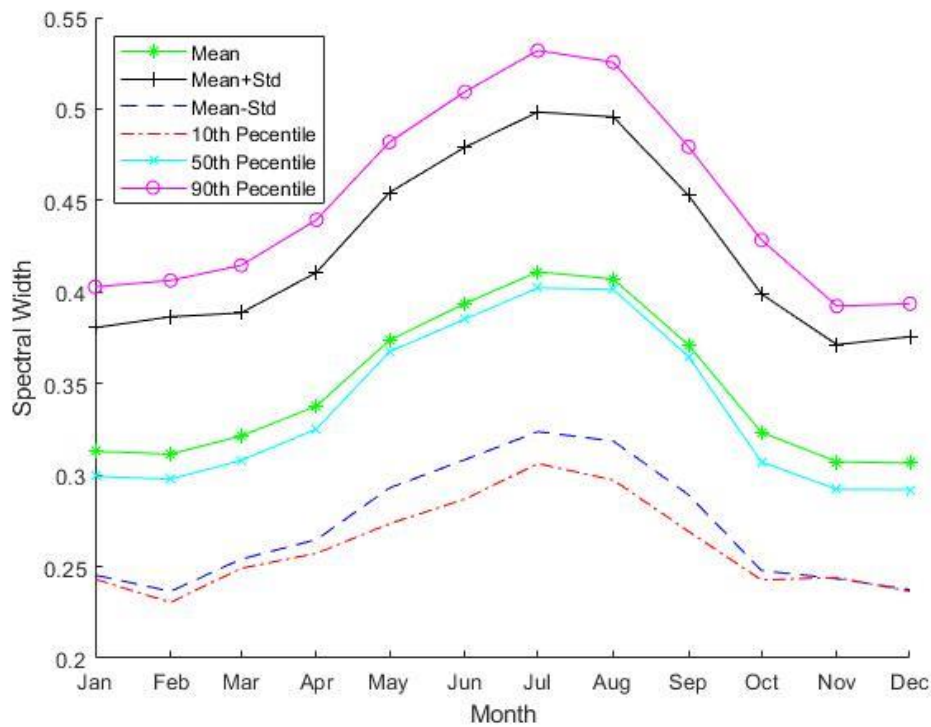


Figure 13: Monthly mean of SWAN spectral width from 1980-2010 at PacWave South

4.4 Monthly cumulative distributions

Monthly cumulative distributions are shown for the characterization parameters to detail the monthly wave resource. A cumulative probability distribution function (CDF) $f(x)$ must equal 0 when the line describing the CDF is at negative infinity, indicating a 0% chance occurrence, and must approach 1 as the line approached positive infinity, indicating a 100% chance occurrence. The steepness of the line indicates the deviations of the data, where a steep curve is indicative of a low deviation.

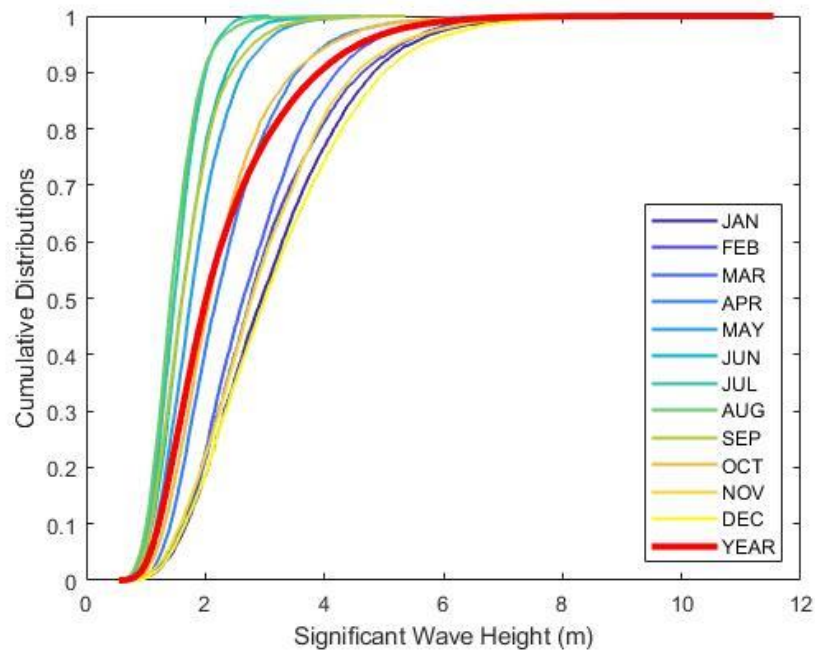


Figure 14: Monthly cumulative distributions of SWAN significant wave height from 1980-2010 at PacWave South

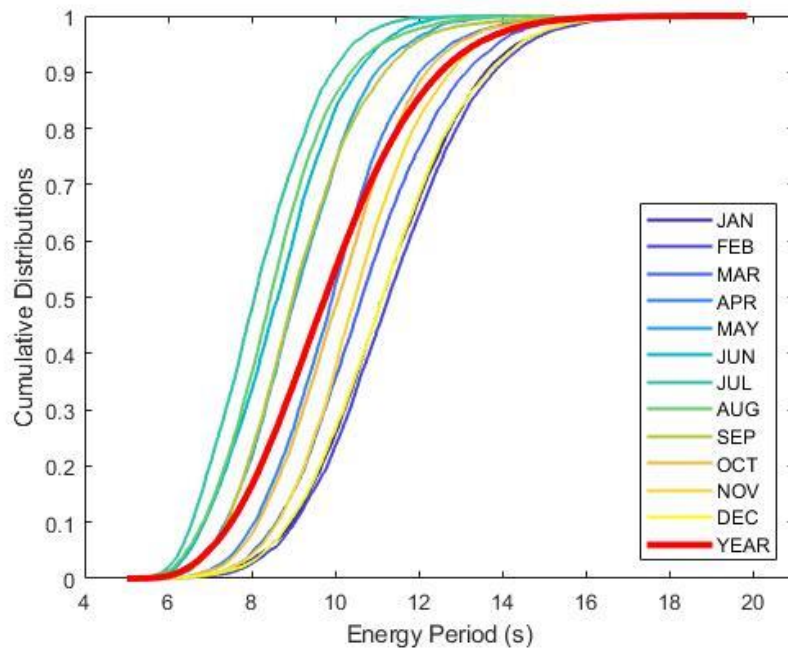


Figure 15: Monthly cumulative distributions of SWAN energy period from 1980-2010 at PacWave South

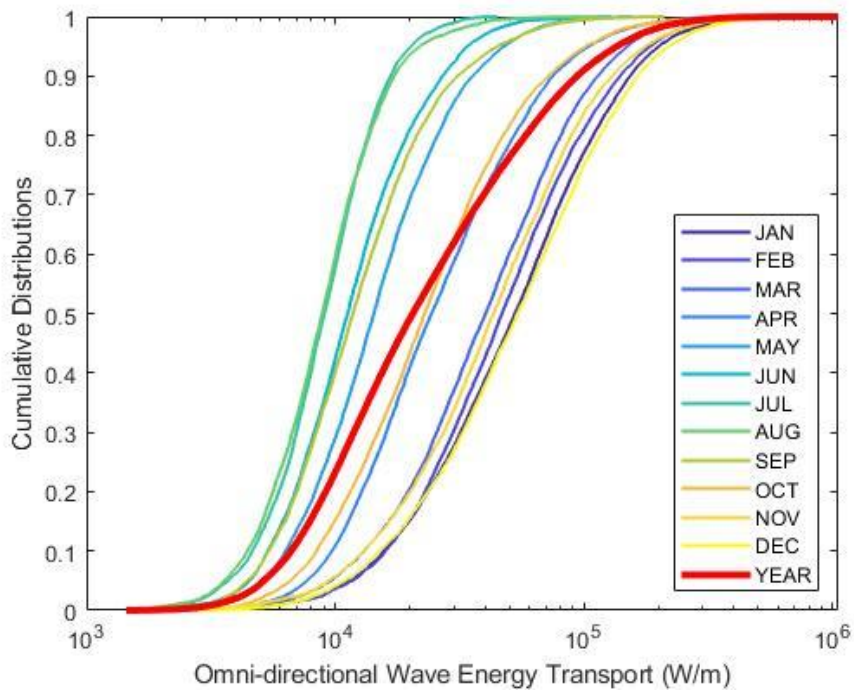


Figure 16: Monthly cumulative distributions of SWAN omni-directional wave energy transport from 1980-2010 at PacWave South. The x-axis is plotted on a logarithmic scale in order to better exhibit the cumulative distribution.

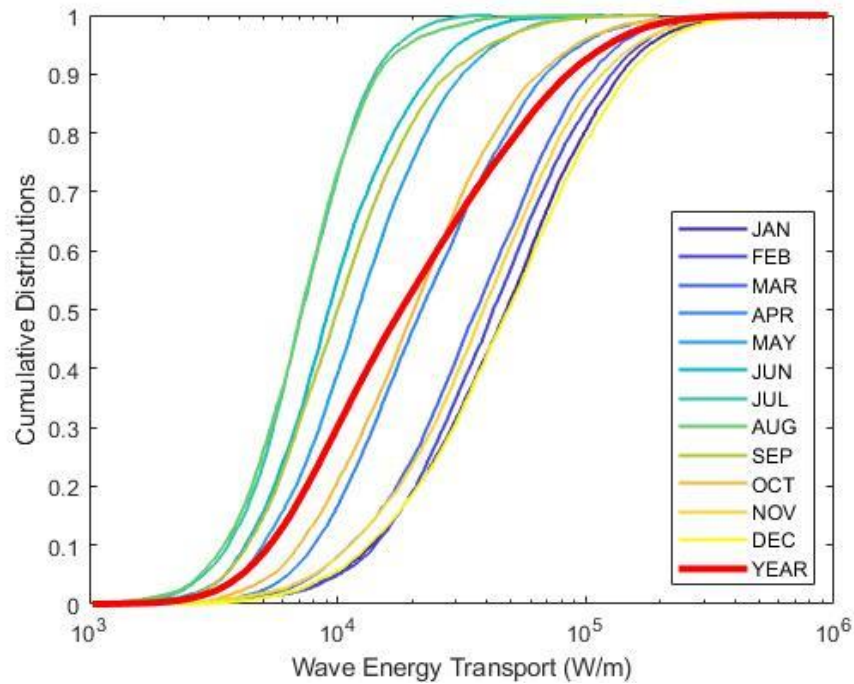


Figure 17: Monthly cumulative distributions of SWAN maximum directionally resolved wave energy transport from 1980-2010 at PacWave South. The x-axis is plotted on a logarithmic scale in order to better exhibit the cumulative distribution.

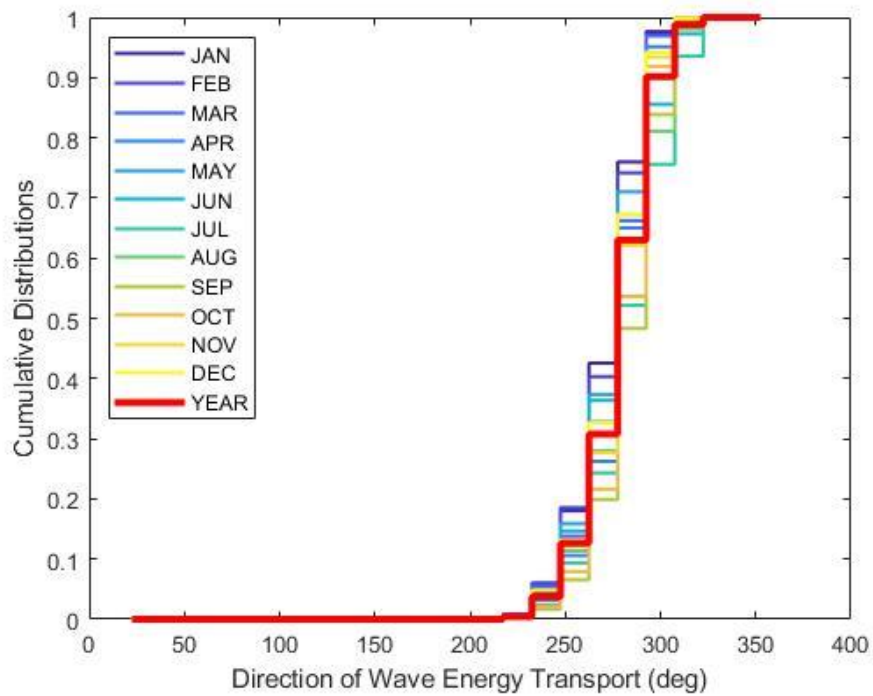


Figure 18: Monthly cumulative distributions of SWAN direction of directionally resolved wave energy transport from 1980-2010 at PacWave South

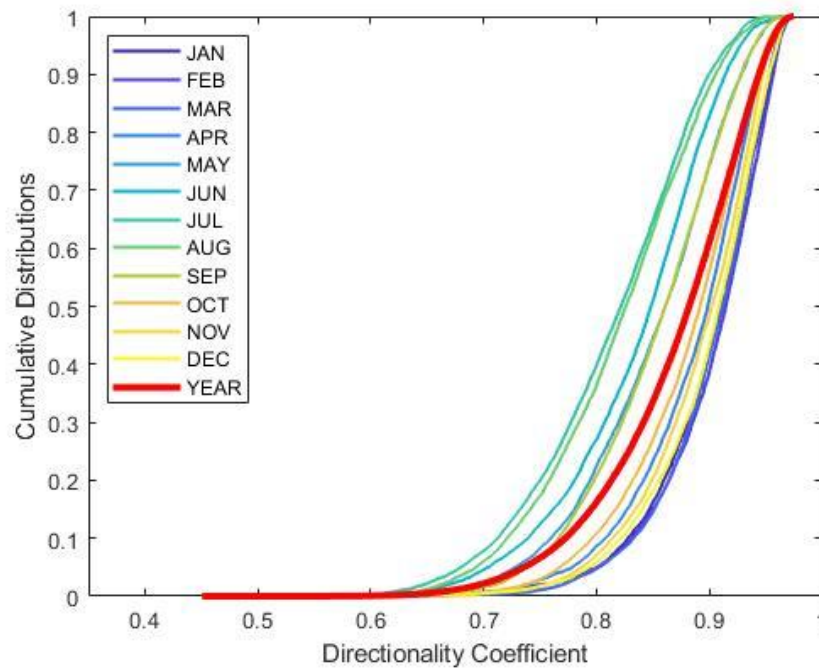


Figure 19: Monthly cumulative distributions of SWAN directionality coefficient from 1980-2010 at PacWave South

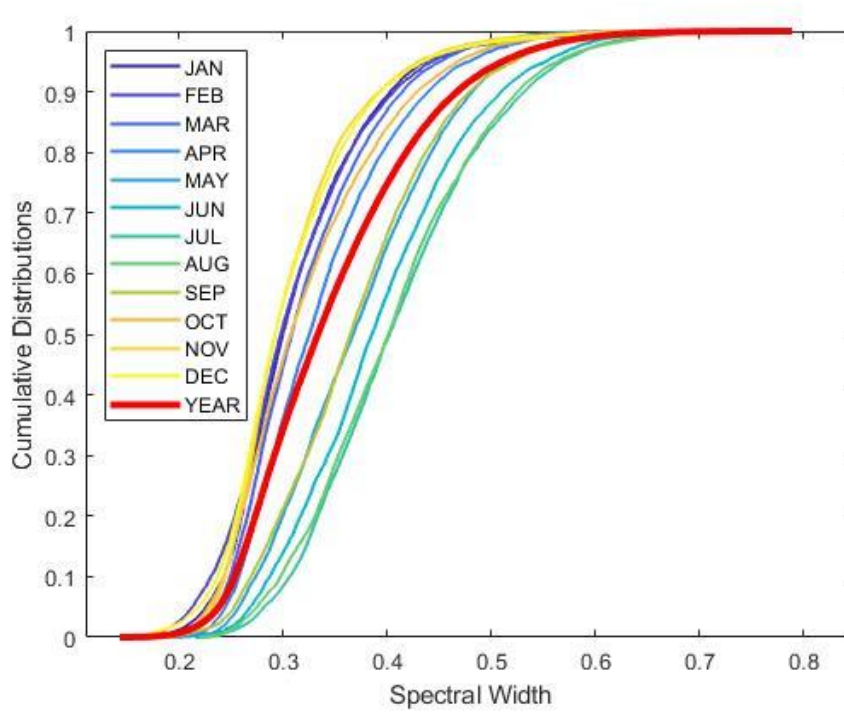


Figure 20: Monthly cumulative distributions of SWAN spectral width from 1980-2010 at PacWave South

5 TEMPORAL FLUCTUATION OF IEC PARAMETERS

Temporal fluctuations of wave parameters are included to highlight the interannual variability of the variables as well as to demonstrate the agreement between the modeled and physically observed data. All plots in Figure 21 show the SWAN calculated parameters from the PNNL hindcast at PacWave South in 2010 compared to the physically observed data at NDBC station 46050 in 2010 (location described in Section 6). This comparison is also included according to the recommendations set by the IEC specification for wave energy resource assessments. For a detailed validation of the SWAN hindcast, please see Wu et al., 2020 [5].

In general, the physically observed data at NDBC 46050 agrees with the modeled data from the PNNL hindcast. There are instances in the direction of maximum directionally resolved wave energy transport plot where NDBC 46050 drops to 0° while the directions in the hindcast vary between 250° and 300° . Additionally, directionality coefficient for the model varies between 1 and 0.6 while physically observed directionality coefficient varies between 0.8 and 0.4. Despite this, all IEC parameters showed good error statistics in model validation [5], indicating that the model has good skill in estimating the IEC parameters.



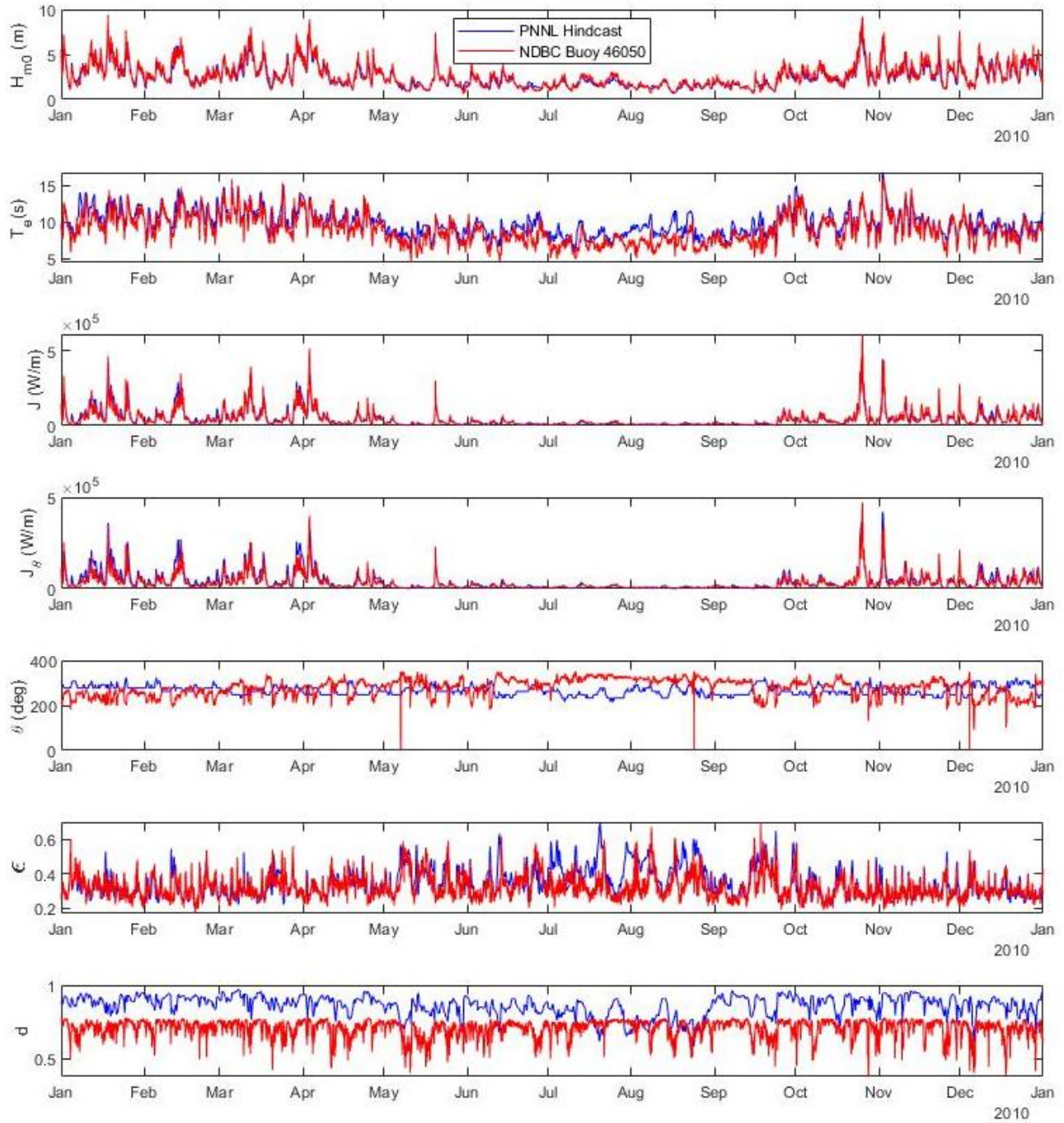


Figure 21: Temporal fluctuation of IEC wave energy parameters for the year 2010. The PNNL hindcast values are representative of the values at PacWave South while the NDBC 46050 values were recorded at its associated location.

6 WIND EFFECT AT PACWAVE

The IEC specification notes that reviewing wind speed and wind direction in the area of interest for wave energy conversion is a valuable addition to a wave resource assessment. The following section offers a general description of the wind field in the PacWave region.

While reporting the seven IEC-required spectral wave quantities for a wave energy resource assessment is descriptive, uncertainty is introduced in wave power predictions when environmental conditions are not adequately taken into account [10]. This effect is under investigation, with researchers attempting to provide additional metrics with which to accurately describe wave energy resource. Robertson et al. has identified wind speed as an additional essential parameter that should be included for a more accurate estimation of wave power [10]. Wave theory describes how waves are affected by wind: wave height grows proportionally to wind speed and duration, thus affecting the amount of energy available in a sea state (i.e. wind generates waves).

Wind data from National Oceanic and Atmospheric Administration (NOAA) National Buoy Data Center (NDBC) stations was analyzed. Wind speed data at NDBC stations is measured by averaging windspeed over an 8-minute period at the height of the offshore buoy anemometers, which is 4.5 m above sea level – which is a relevant elevation for most WEC systems. Figure 22 shows some of the available regional NDBC buoy data in Oregon, Southern Washington, and Northern California. The boxed area represents the specific PacWave region and associated NDBC stations, further described in Figure 23.

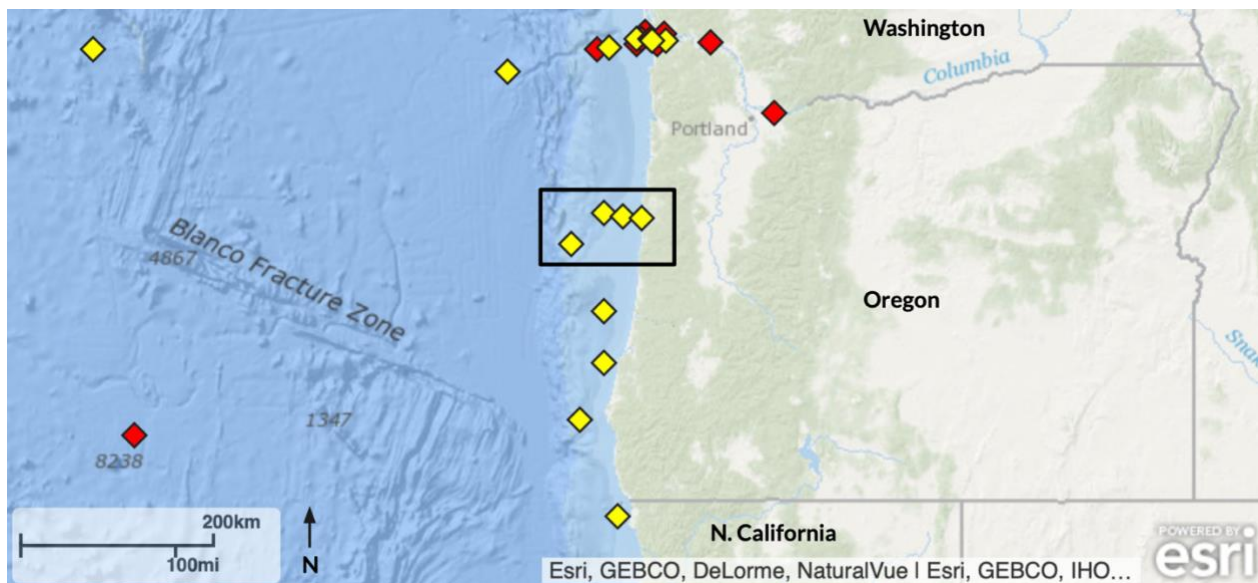


Figure 22: Regional NDBC station locations. Red diamonds indicate stations with no recent data collected, while yellow indicates ongoing data collection at the location. The black box denotes the specific location of the PacWave wave energy test site and associated NDBC stations.

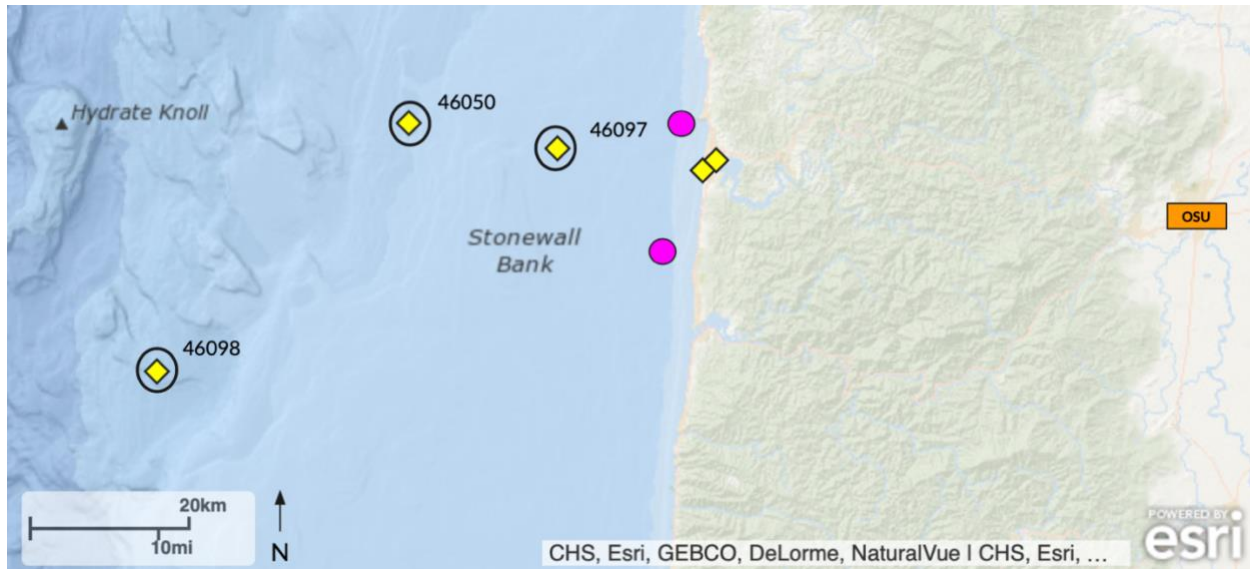


Figure 23: Locations of NDBC buoys from which wind data was analyzed, in reference to the location of PacWave and OSU

In Figure 23, yellow diamonds denote NDBC buoy stations and the red circles indicate the stations used in this report. The pink circles show the approximate locations of PacWave North and South sites from top to bottom respectively, off the coast of Newport. The orange box represents the location of Oregon State University in Corvallis.

The distributions of wind speed and direction were analyzed from NDBC stations 46097, 46098, and 46050 and plotted in Figure 24 through Figure 26. Station 46097 recorded data from 2016 through 2019, station 46098 from 2016 through 2017, and station 46050 from 2014 through 2016. Each distribution was fitted with a Weibull distribution, which is the expected distribution for wind speed since it proves to be a good approximation for this type of measurement [11].

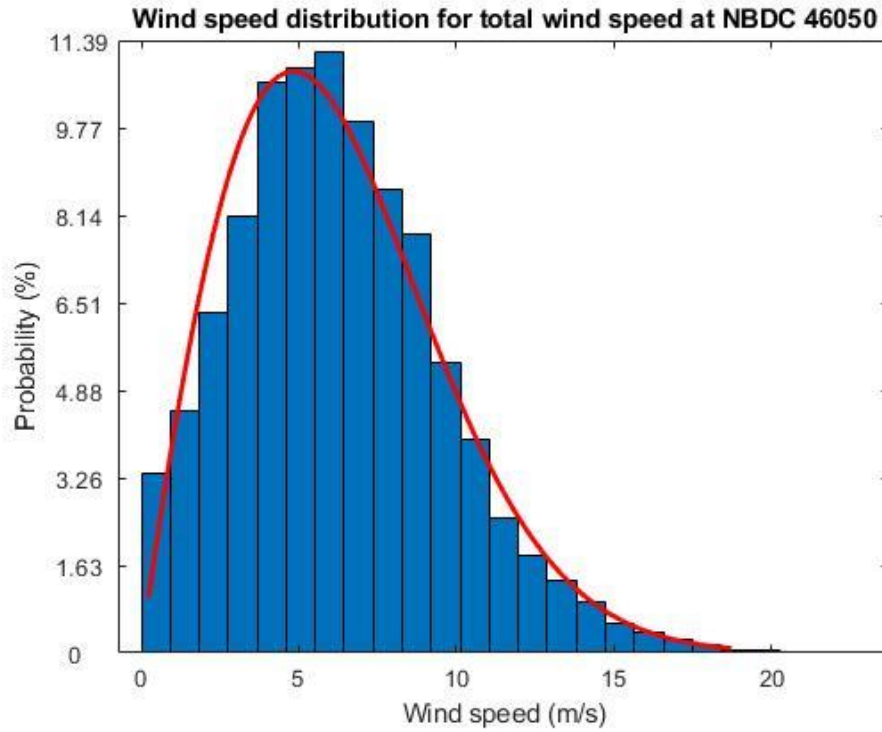


Figure 24: Distribution of wind speed at NDBC 46050 with a Weibull distribution fit

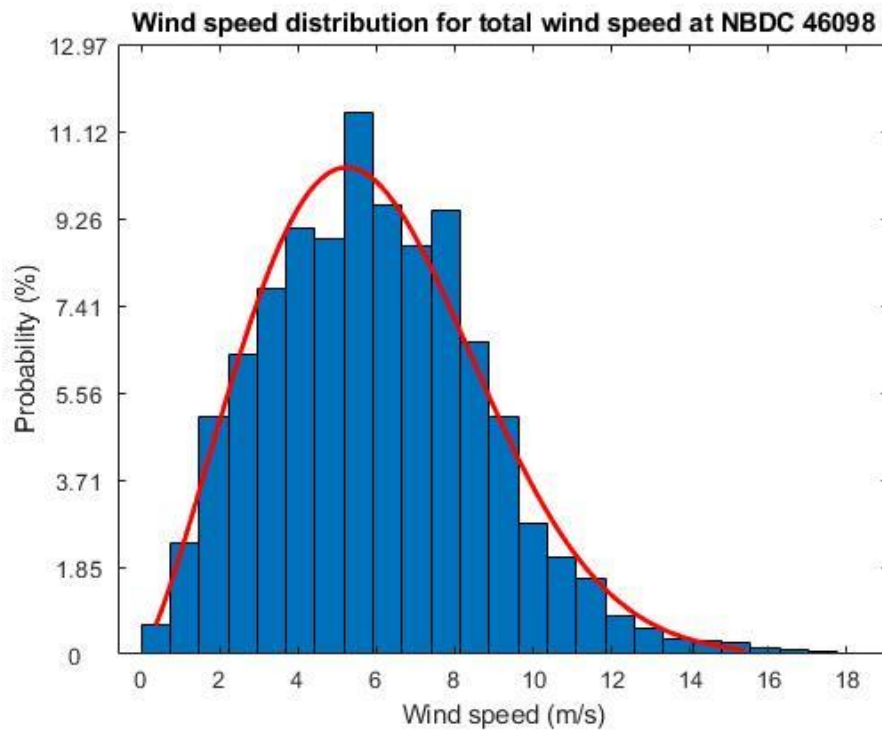


Figure 25: Distribution of wind speed at NDBC 46098 with a Weibull distribution fit

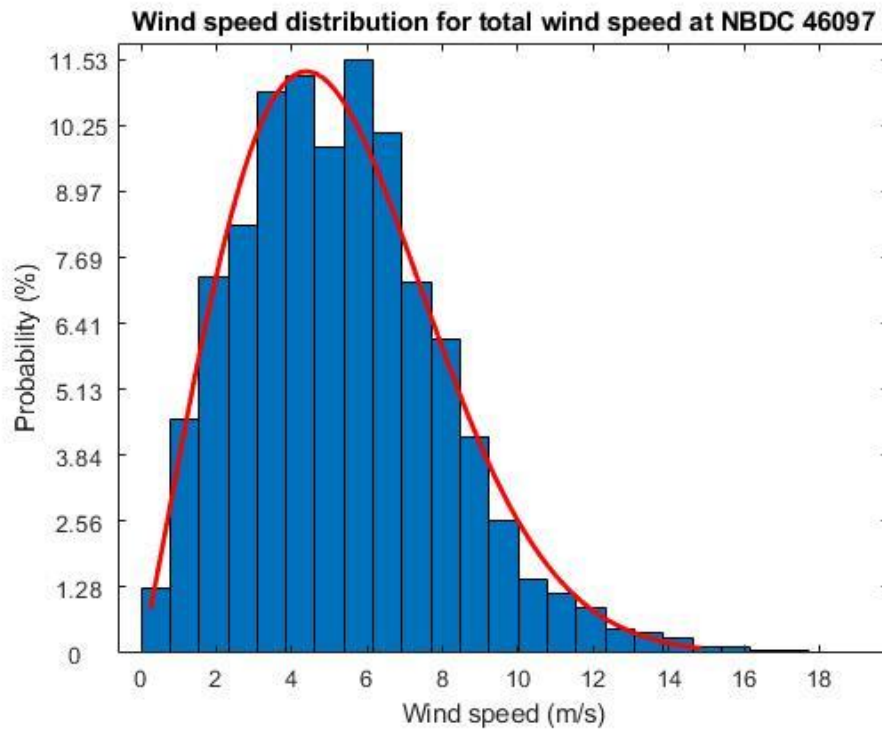


Figure 26: Distribution of wind speed at NDBC 46097 fitted with a Weibull distribution fit

Across the three NDBC stations, the majority of wind speeds are in the 4-8 m/s range, accounting for the highest probability of occurrence. Maximum values of wind speed are 18 m/s per each of the stations. The average wind speed at NDBC 46050 is 6.27 m/s; average windspeed at NDBC 46097 is 5.32 m/s; and average windspeed at NDBC 46098 is 5.98 m/s. The boxplot in Figure 27 describes the range of values measured at the NDBC stations.

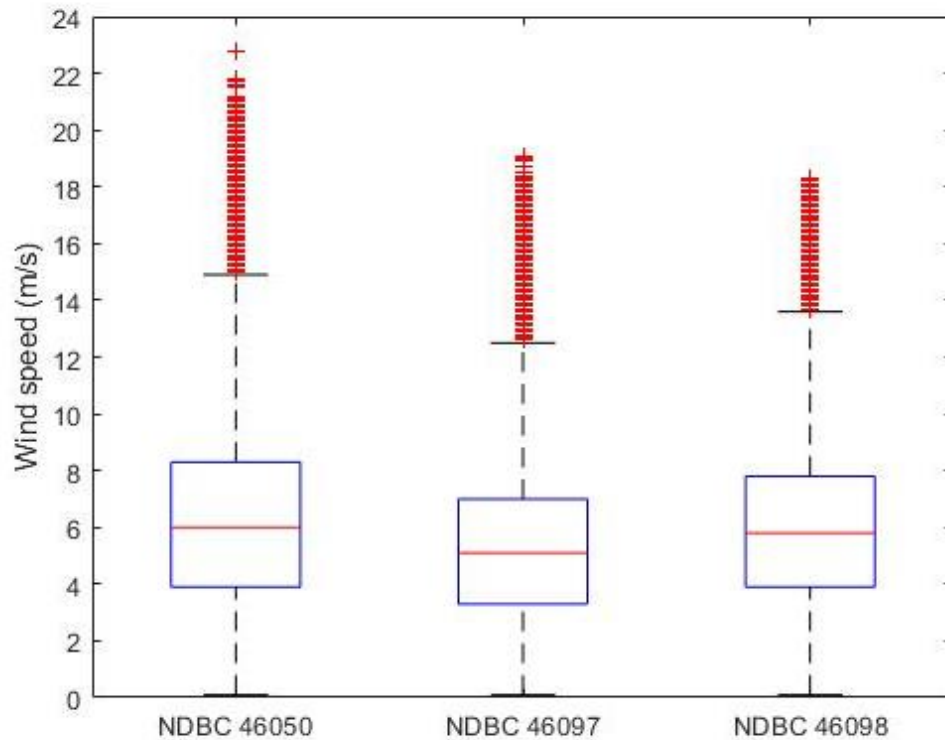


Figure 27: Box and whisker plot describing the wind speeds at NDBC stations near PacWave. Shown in the plot are extreme outlier values, non-extreme minima and maxima, median values (50th percentiles), and 25th and 75th percentile values.

The lower and upper limits of the interquartile range (IQR) denote the 25th and 75th percentiles respectively. Whiskers lead to the most extreme, non-outlier values, and crosses are outlier values. The red line indicates the median value of the dataset, which will fall somewhere within the IQR; at least half of the data is less than or equal to the median and at least half is greater than or equal to it.

The median wind speeds at NDBC 46050, 46097, and 46098 are 6 m/s, 5.1 m/s, and 5.8 m/s respectively; maximum non-outlier wind speeds are 15 m/s, 12.5 m/s, and 13.6 m/s respectively; minimum non-outlier wind speeds are 0.1 m/s at each station. Outliers range from 18 m/s to 23 m/s between the three sites. Figure 27 provides an extensive description of the wind speeds measured near the PacWave sites.

NDBC 46097 has wind data collected from 2016 through 2019 and is closest to the PacWave sites, therefore the station's data was used for representing the directional distribution of the wind speed, as shown in Figure 28. NDBC 46097 measured wind speed and direction measurements from 2016 through 2019 and is located closest to the PacWave sites, as demonstrated in Figure 23. The percentages indicate the frequency at which each bin occurs.

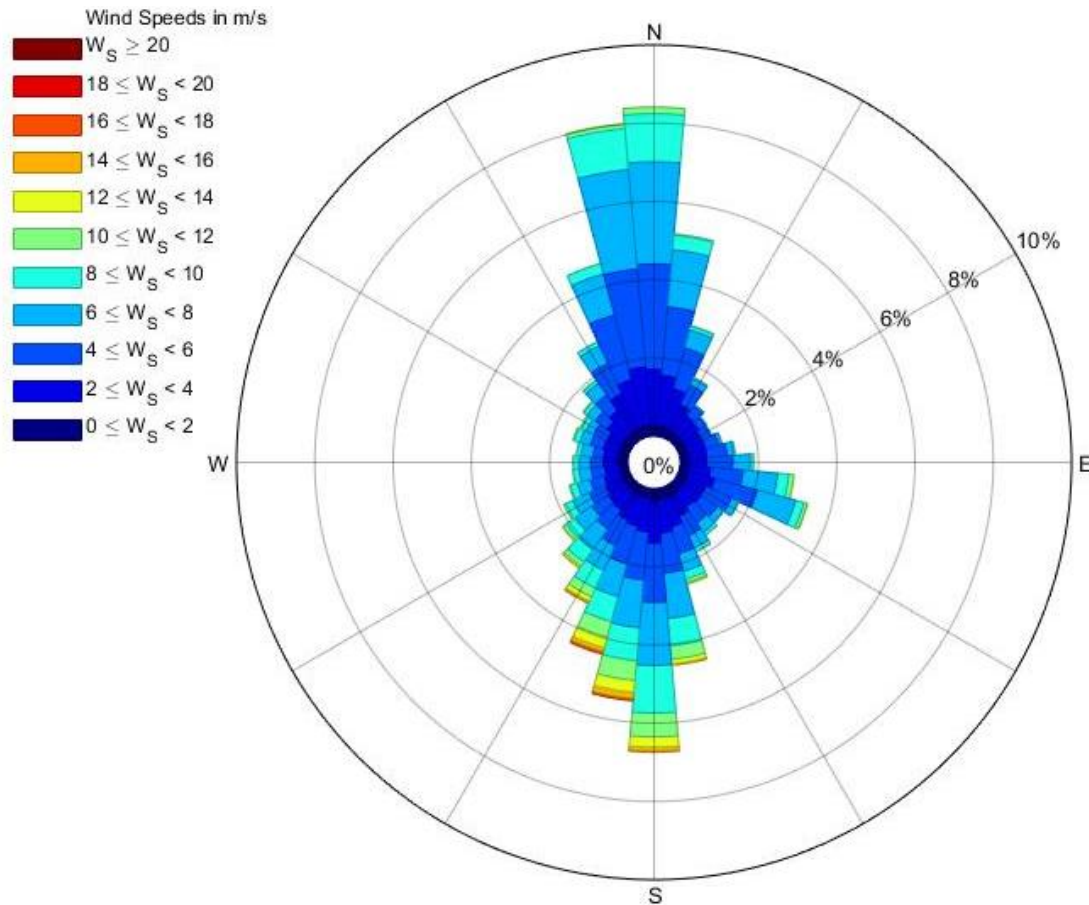


Figure 28: Wind rose distribution for wind speed at NDBC 46097 from 2016-2019

Wind direction at the NDBC stations is measured as the wind is coming from degrees clockwise from 0° North. As expected, the winds come predominately from the north and south. The inclusion of wind speed, among other environmental conditions, decreases uncertainty when comparing modeled data to physically observed sea state data [10].

7 EXTREME ENVIRONMENTAL CONTOURS

When determining the site characteristics for potential wave energy conversion, it is recommended by the IEC to take into consideration extreme sea state conditions. 50-year and 100-year environmental contours were used in this section to describe potential extreme sea states at the PacWave sites. WEC developers may run into issues at the PacWave site due to large waves that occur in the winter months, highlighting the need to ensure survivability of WEC devices.

100-year storm events have a likelihood of 1% per year occurrence, whereas 50-year events have a 2% likelihood of occurrence per year. The analysis corresponding to extreme wave

events in this section is based on Yang et al. (2020), and should be explored for further detail [4]; the environmental contour data used in this report is from PNNL.

Figure 29 and Figure 30 detail the extreme environmental contours in the PacWave region compared to the hindcast predictions. Extreme values at $44^{\circ}36'7.56''\text{N}$ and $124^{\circ}13'55.2''\text{W}$ were chosen to compare to the PacWave hindcast measurements, as this location was closest to the actual PacWave South longitude and latitude (i.e. 1.5 miles northwest of PacWave South).

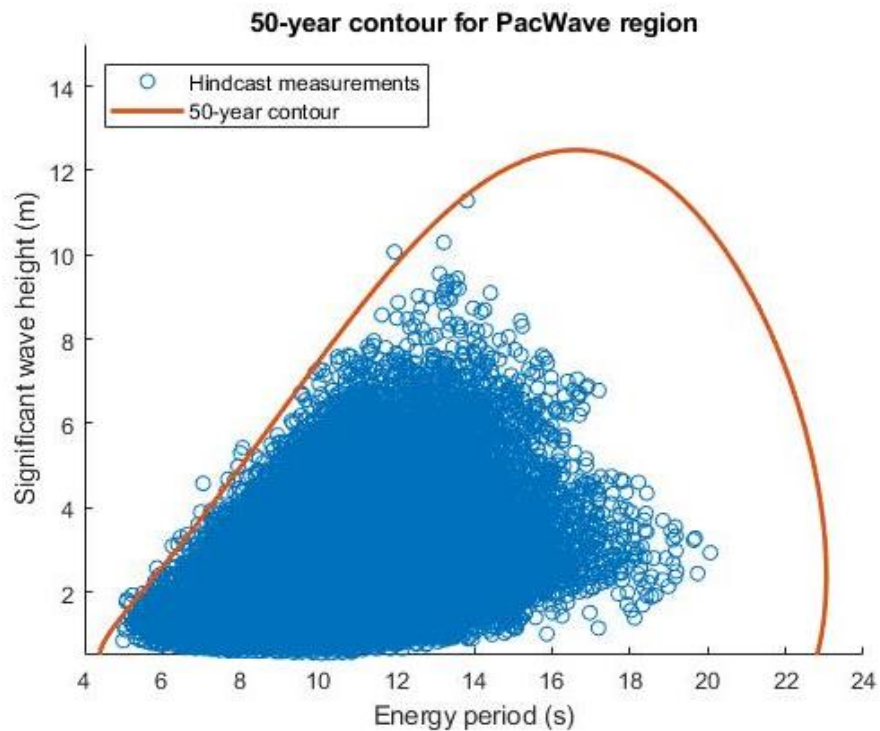


Figure 29: 50-year extreme environmental contour for the PacWave region compared to hindcast measurements recorded for PacWave South from 1980-2010

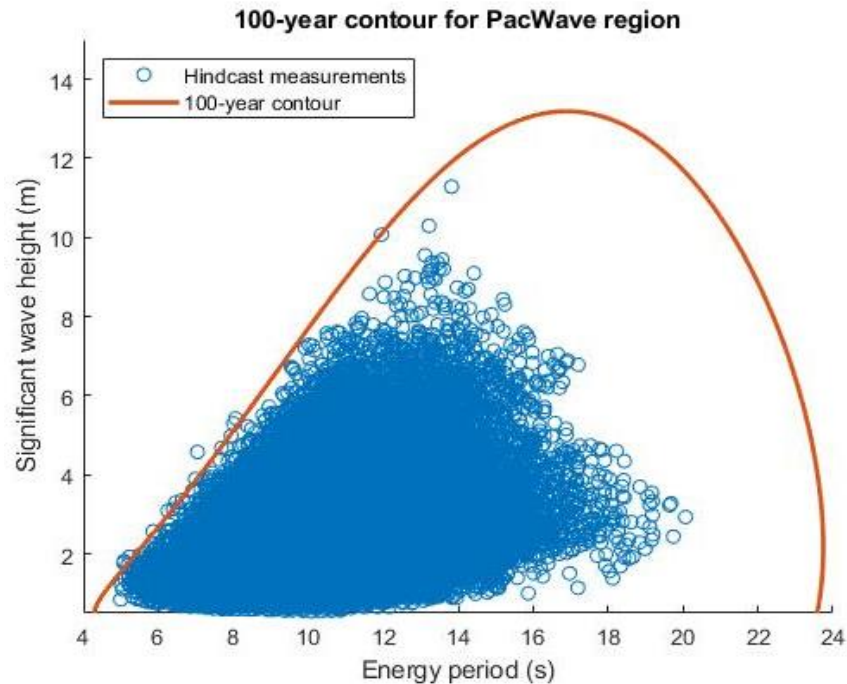


Figure 30: 100-year environmental contour for the PacWave region compared to hindcast measurements recorded for PacWave South from 1980-2010

In both Figure 29 and Figure 30 there are hindcast values that are aligned on the contour lines, which was expected since the dataset analyzed in this report encompasses 31 years, throughout which extreme sea states are statistically bound to occur. This reinforces the advantage of using a long-term dataset. The right-hand portions of each plot lack measurements because the hindcast dataset is not 50 nor 100 years long, during which times the more extreme values would be more likely to occur.

The maximum wave height – energy period combination is about the same for both the 100-year and 50-year contours. The peak of the 50-year contour occurs at a wave height of 12.49 m and energy period of 16.68 s while the 100-year contour peaks at a wave height of 13.19 m and energy period of 16.85 s. From 1980-2010, the hindcast did not measure any values possessing this combination of extreme values.

Extreme environmental analysis is included in this report in order to describe the sea state conditions that may occur at the PacWave sites. Survivability is of concern for WEC developers as high, steep, and breaking waves tend to damage WEC devices, especially at increased frequencies [11].

8 OPERATION & MAINTENANCE WINDOWS

Figure 31 characterizes the average number of single-day weather windows per year available for developers to access and perform operation and maintenance (O&M) at PacWave South. The cumulative amount of days with significant wave height less than 1.5 meters and peak period above 8 s from 1980-2010 are totaled on the plot [12] — these threshold operations windows are based on data from the Navy Wave Energy Test Site in Hawaii and are vessel specific. As expected, throughout this analysis, the summer months yield more optimal conditions for O&M than winter months. The peak for average individual day windows for O&M at PacWave South is 4.6 days in August per year between 1980 and 2010. The months from November through March see less than one full day on average per year available for O&M.

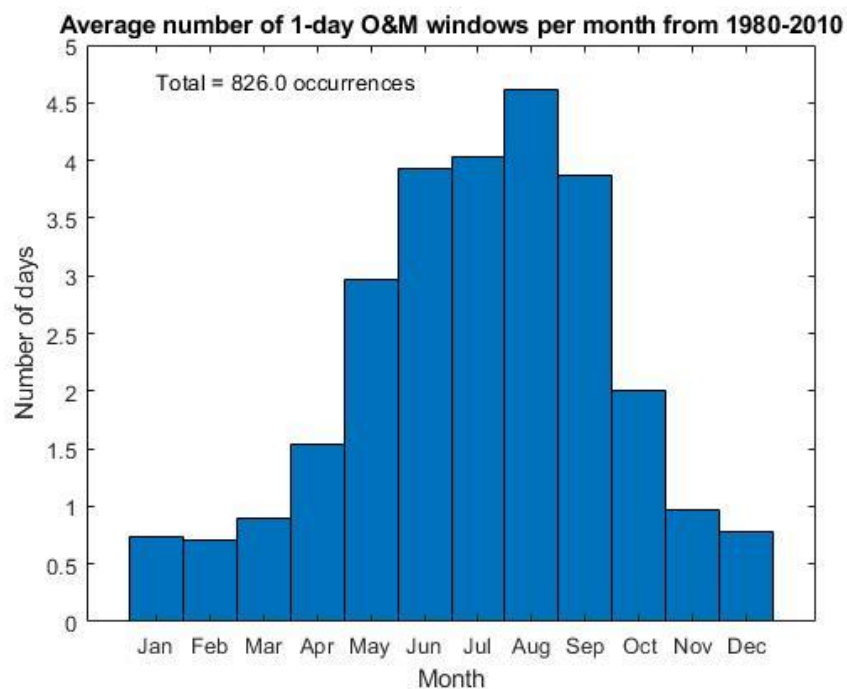


Figure 31: Average number of days with wave height less than 1.5 m and peak period above 8 s available for O&M from 1980-2010 at PacWave South

The average number of 2-day, 3-day, and 5-day weather windows available per year for O&M are shown in Figure 32, Figure 33, and Figure 34 respectively. As expected, summer months June, July, and August allow more opportunity for O&M than winter months. The peak number of 2-day, 3-day, and 5-day windows at PacWave South is 2.4, 1.3, and 0.5 occurrences respectively, all taking place in August. Table 1 and Table 2 describe the average amount of window occurrences per year and month respectively.

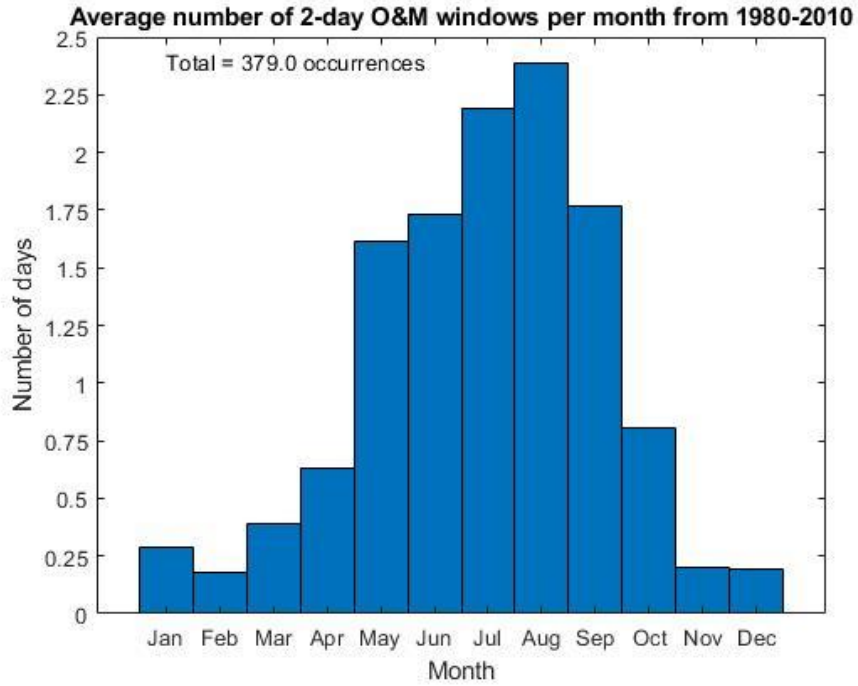


Figure 32: Average number of 2-day windows with wave height less than 1.5 m and peak period above 8 s for O&M from 1980-2010 at PacWave South

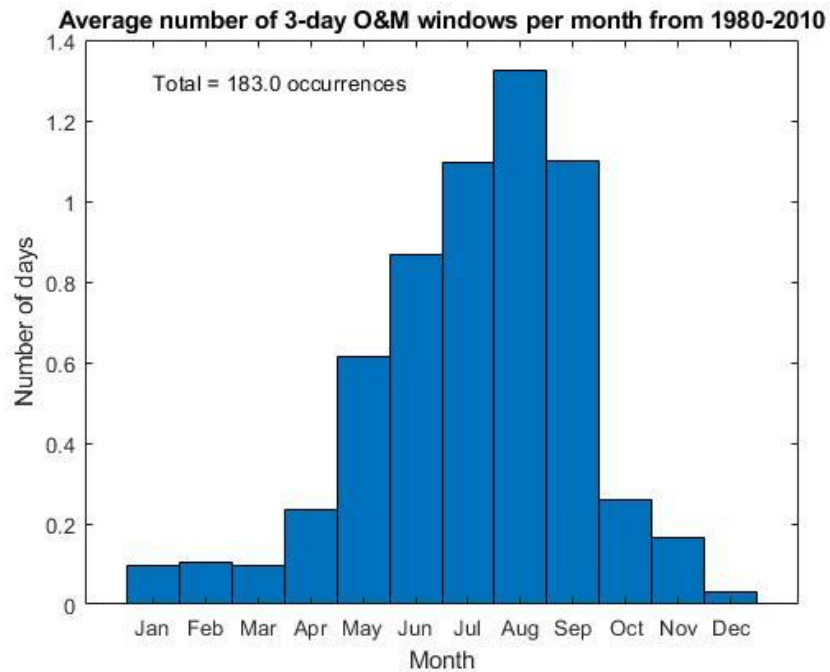


Figure 33: Average number of 3-day windows with wave height less than 1.5 m and peak period above 8 s for O&M windows from 1980-2010 at PacWave South

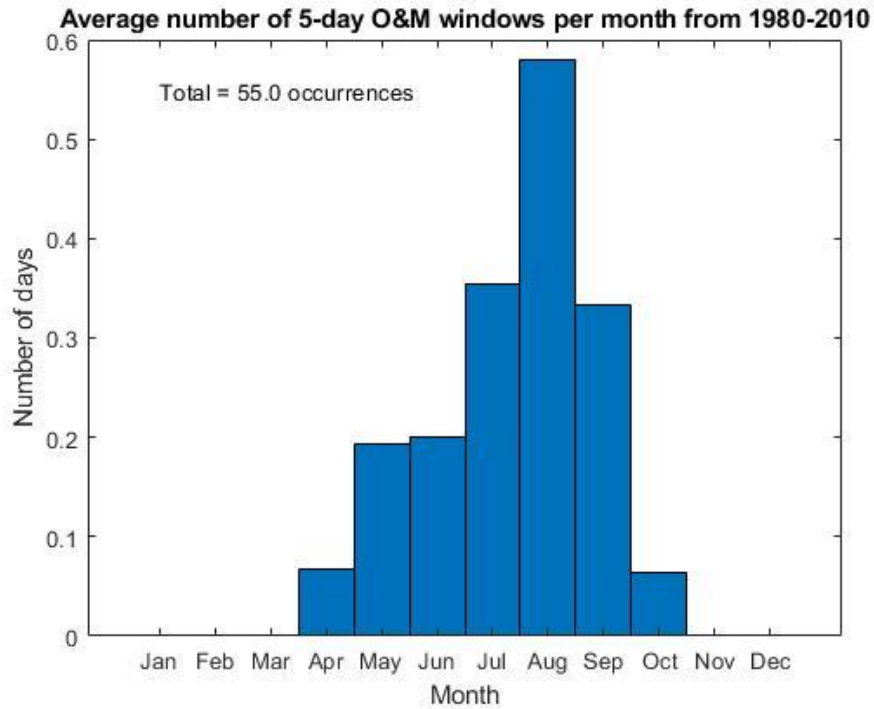


Figure 34: Average number of 5-day windows with wave height less than 1.5 m and peak period above 8 s for O&M from 1980-2010 at PacWave South

	1-day windows	2-day windows	3-day windows	5-day windows
North	28	13	6.5	2
South	27	12	6	2

Table 1: Average O&M windows per year from 1980-2010

	Jan	Feb	Mar	Apr	May	Jun	Jul	Aug	Sep	Oct	Nov	Dec
1-day windows	0.7	0.7	0.9	1.5	3.0	4.0	4.0	4.6	3.8	2	1.0	0.8
2-day windows	0.3	0.2	0.4	0.6	1.6	1.7	2.2	2.4	1.8	0.8	0.2	0.2
3-day windows	0.1	0.1	0.1	0.2	0.6	0.9	1.1	1.3	1.1	0.3	0.2	0
5-day windows	0	0	0	0.1	0.2	0.2	0.4	0.6	0.3	0.1	0	0

Table 2: Average number of O&M windows per month from 1980-2010 at PacWave South

Box and whisker plots were created for the various O&M window durations in order to provide a comprehensive look at the probability of occurrence of satisfactory sea state conditions. The number of days available per month within the O&M conditions were recorded for the time period. Figure 35 through Figure 38 describe the interannual variability of O&M on a monthly basis from 1980-2010.

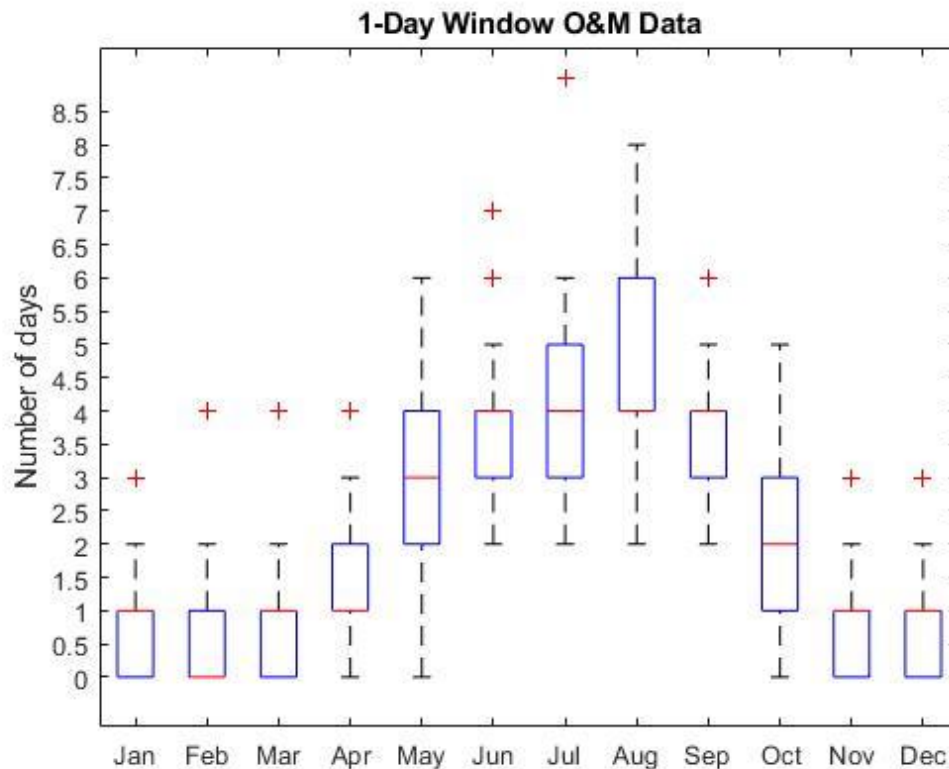


Figure 35: Box and whisker plot describing the 1-day window O&M data at PacWave South. Shown in the plot are extreme outlier values, non-extreme minima and maxima, median values (50th percentile values), and 25th and 75th percentile values.

Figure 35 shows the range of occurrences of 1-day O&M windows from 1980-2010. The winter months from November through March consistently have median values that align with either the 25th or 75th percentile, indicated by a red line marking the outside of the IQR box. This result is due to increased occurrence of such values in the middle of the monthly dataset. There is a non-outlier maximum of two days which occurred during these months in certain years. The summer months have non-outlier maxima of at least two days greater than the 75th percentile and centered median values in the IQR, except for August. Again, this is due to the fact that 4 days was recorded the most frequently in the middle of the August dataset.

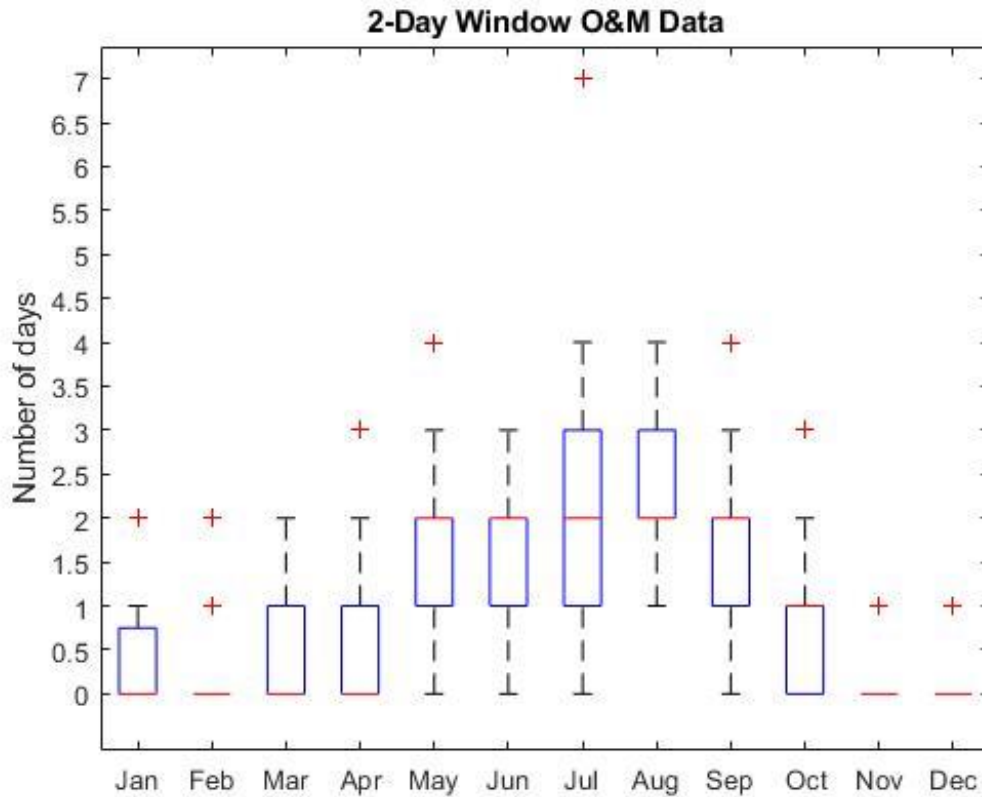


Figure 36: Box and whisker plot describing the 2-day window O&M data at PacWave South. Shown in the plot are extreme outlier values, non-extreme minima and maxima, median values (50th percentile values), and 25th and 75th percentile values.

Figure 36 describes the box and whisker plot data associated with the spread of occurrences of 2-day windows for O&M at PacWave South. As expected, there are fewer occurrences of this window type across the months. Winter months February, November, and December lack an IQR box as 0 is the most recorded window occurrence, with outliers occurring at 1 and 2 days depending on the month. From May through September, the median value for occurrences of 2-day windows is 2, with non-outlier maxima ranging from 3 to 4 occurrences and non-outlier minima between 0 and 1 occurrences. From 1980-2010, there is always at least one 2-day O&M window occurring in August according to the hindcast.

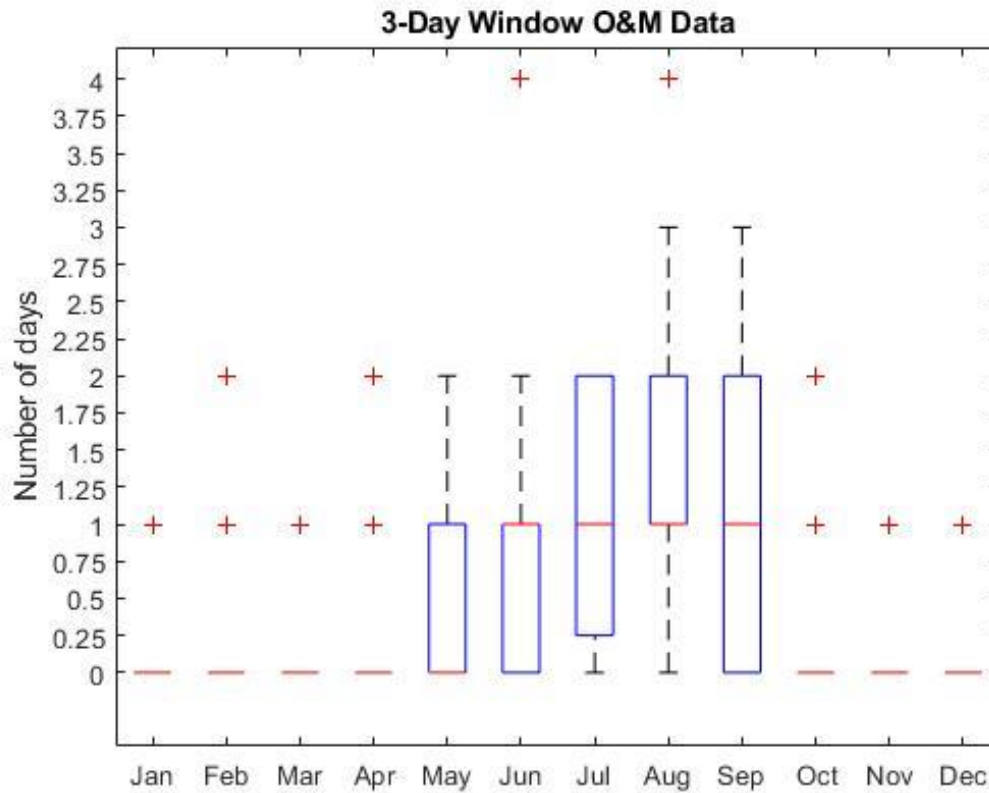


Figure 37: Box and whisker plot describing the 3-day window O&M data at PacWave South. Shown in the plot are extreme outlier values, non-extreme minima and maxima, median values (50th percentile values), and 25th and 75th percentile values.

3-day windows for O&M purposes are sparser from 1980-2010 according to the hindcast. Figure 37 indicates that half the months in a year rarely see an opportunity for 3-day windows with favorable sea state conditions. Months between November and April have outliers ranging from 1 to 2 occurrences and medians of 0 occurrences, lacking an IQR box. From months May through September, the median value of 3-day window occurrences is 1. May and June have non-outlier maxima of 2 occurrences; July and August have non-outlier minima of 0 occurrences. Additionally, August has a non-outlier maximum of 3 and an outlier of 4 occurrences, with a 75th percentile value of 2 occurrences. According to Figure 37, September has an equal probability of window occurrence as July. October has a median of 0 occurrences and an 75th percentile value of 1 occurrence and a non-outlier maximum of 2 occurrences. In summary, 3-day windows are more likely to occur between July and September.

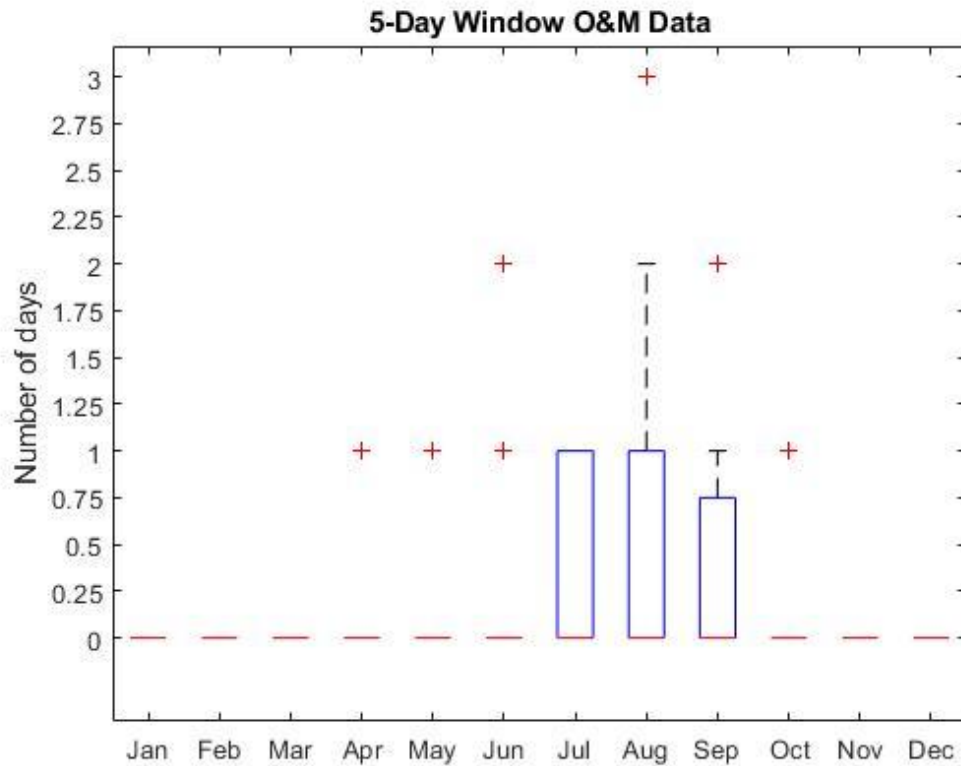


Figure 38: Box and whisker plot describing the 5-day window O&M data at PacWave South. Shown in the plot are extreme outlier values, non-extreme minima and maxima, median values (50th percentiles), and 25th and 75th percentile values.

As expected, Figure 38 demonstrates there are few likely occurrences of 5-day windows available from 1980-2010 in any given month. November through March do not have a recording of a 5-day window, indicated by medians equal to 0 and a lack of outlier values. April, May, June, and October also have medians equal to 0 with outliers between 1 and 2 occurrences. Months July through September also have median values equal to 0 occurrences, with 75th percentile values of 1 and 0.75 respectively. August has a non-outlier maximum of 2 occurrences and an outlier of 3 occurrences of this window type.

The analysis of box and whisker plots for O&M purposes allows for deeper look at potential favorable sea state window opportunities. The range of occurrences available per window type per month, maximum and minimum, median, and outlier occurrences were investigated and presented in this report in order to allow for better assessment and planning for O&M on WEC devices at PacWave.

9 CONCLUSIONS

This report contains a detailed analysis of wave energy resource at the PacWave South and North (shown in Appendix) sites off the coast of Newport, Oregon, utilizing on a 32-year (1980-2010) hindcast developed by the PNNL and based on the International Electrotechnical Commission technical specifications. Bivariate histograms of significant wave height and energy provide a visual description of the variety of sea states occurring at the PacWave sites. The highest mean annualized wave energy transport sea state occurred a total of 231 hours with a significant wave height of 2.75 m and an energy period of 10.5 s at PacWave South. The wave rose illustrates the major directions from which the directionally resolved wave energy transport propagates at PacWave South; the majority of directionally resolved wave energy transport comes from the west.

The monthly means, standard deviations, 10th, 50th, and 90th percentiles of the IEC recommended wave characteristics were calculated and plotted to display the variation, upper and lower limits, and potential skewness of the dataset. It was confirmed that the dataset used in this analysis is skewed, as the mean value of each parameter (except for directionality coefficient) is greater than the median, or the 50th percentile line throughout most of the year. This is typical for sea states as extreme events do not frequently occur throughout the year, but rather are concentrated in the winter months. In the analysis of significant wave height, energy period, and omni-directional and maximum directionally resolved wave energy transports the values increase in the winter months and decrease in the summer, which is attributed to an increase in storms during the winter. The interannual variability is apparent and easily visible in the plots in this section.

In addition to the monthly statistics representation, monthly cumulative distributions were shown to provide greater detail of the wave resource parameters per month throughout the hindcast. Temporal fluctuations were shown for the year 2010 of the PNNL hindcast and were compared to physically observed data recorded at NDBC 46050. The purpose of this assessment was to give a better idea of inter-annual variability of wave resource parameters, and to demonstrate the agreement between physically observed data and the modeled data.

Wind effects at PacWave were investigated in order to demonstrate the necessity of broadening the basis from which a complete wave energy resource assessment is made. A boxplot was created to show the range of measurements recorded at the NDBC stations. Wind direction and speed data from NDBC 46097 was analyzed to show a profile of the winds dominating the field in the PacWave region.

Extreme environmental contours were shown based on the IEC recommendation to include extreme sea state information in a wave energy resource assessment. Doing so is valuable to a wave energy resource assessment as WEC developers must consider extreme sea states when necessarily preparing WECs for survival in potentially harsh ocean environment. The value of

analyzing a long-term dataset is reinforced in this section, as the hindcast period from 1980-2010 is considered long-term. The plots in this section infer that wave height and energy period values corresponding to 50- and 100-year extreme sea state values would occur during the 30 years. The maximum extreme wave height and energy period for the 50-year contour are predicted to be 12.49 m and 16.68 s respectively. The 100-year contour yields a maximum wave height of 13.19 m and energy period of 16.85 s.

To provide operation and maintenance (O&M) information for the PacWave sites to parties of interest, the significant wave height and peak period data were filtered to only include complete days of measurements where H_{m0} was less than 1.5 m and T_p was greater than 8 s. The number of full days providing these conditions were normalized on a yearly basis to give an idea of the typical availability throughout a year. Tables were created to show the specific breakdown of days available per year and per month by window length. August was overwhelmingly found to be the optimal month to conduct O&M, as it had the maximum amount of window availability per year. Box and whisker plots were also provided to allow a greater understanding of window availability at PacWave. As expected, 5-day windows have the least likelihood of occurrence, followed by 3-day, 2-day, and single day windows respectively. July, August, and September consistently prove to be the most favorable months in terms of appropriate sea state conditions for O&M.

7 REFERENCES

- [1] A. Cornett, “A global wave energy resource assessment,” *Sea Technol.*, vol. 50, no. 4, pp. 59–64, 2008.
- [2] P. Lenee-Bluhm, R. Paasch, and H. T. Özkan-Haller, “Characterizing the wave energy resource of the US Pacific Northwest,” *Renew. Energy*, vol. 36, no. 8, 2011, doi: 10.1016/j.renene.2011.01.016.
- [3] G. García-Medina, H. T. Özkan-Haller, and P. Ruggiero, “Wave resource assessment in Oregon and southwest Washington, USA,” *Renew. Energy*, vol. 64, 2014, doi: 10.1016/j.renene.2013.11.014.
- [4] Z. Yang, G. García-Medina, W.-C. Wu, and T. Wang, “Characteristics and variability of the nearshore wave resource on the U.S. West Coast,” *Energy*, vol. 203, p. 117818, 2020, doi: 10.1016/j.energy.2020.117818.
- [5] W. C. Wu, T. Wang, Z. Yang, and G. García-Medina, “Development and validation of a high-resolution regional wave hindcast model for U.S. West Coast wave resource characterization,” *Renew. Energy*, vol. 152, 2020, doi: 10.1016/j.renene.2020.01.077.
- [6] International Electrotechnical Commission, *Marine energy: wave, tidal and other water current converters. Part 101, Wave energy resource assessment and characterization.* .
- [7] Delft, “USER MANUAL SWAN - Cycle III version 40.72AB,” *Cycle*, p. 125, 2009.
- [8] C. xxx V. K. Prasada Rao, “Spectral width parameter for wind-generated ocean waves,” *Proc. Indian Acad. Sci. - Earth Planet. Sci.*, vol. 97, no. 2, pp. 173–181, 1988, doi: 10.1007/BF02861852.
- [9] P. Ruggiero, P. D. Komar, and J. C. Allan, “Increasing wave heights and extreme value projections: The wave climate of the U.S. Pacific Northwest,” *Coast. Eng.*, vol. 57, no. 5, pp. 539–552, 2010, doi: 10.1016/j.coastaleng.2009.12.005.
- [10] B. Robertson, H. Bailey, and B. Buckham, “Resource assessment parameterization impact on wave energy converter power production and mooring loads,” *Appl. Energy*, vol. 244, 2019, doi: 10.1016/j.apenergy.2019.03.208.
- [11] M. R. Hashemi and S. P. Neill, *Fundamentals of Ocean Renewable Energy*, 1st ed. Joe Hayton, 2018.
- [12] N. Li, “WETS Program Review and Workshop,” in *Numerical Wave Modeling and Data Analysis for WETS*, 2020.

APPENDIX A: PACWAVE NORTH WAVE RESULTS

A.1 Annual histogram of sea state occurrences

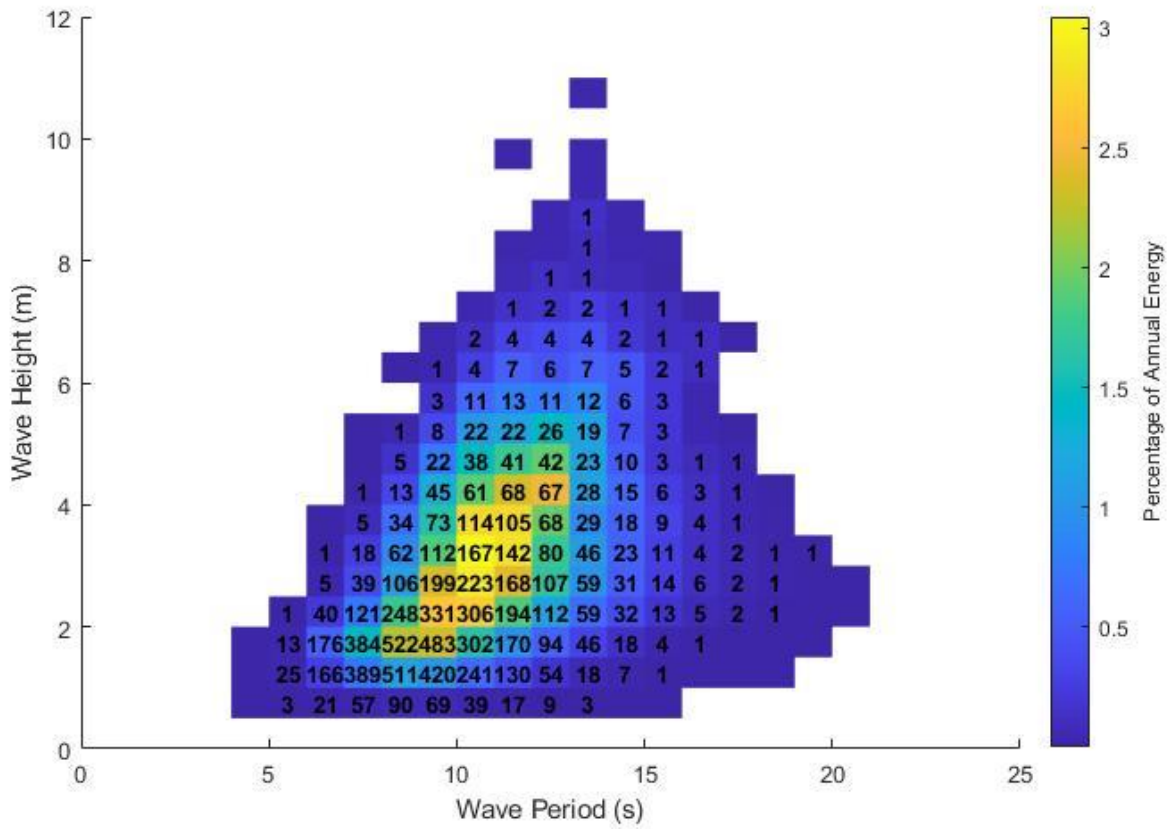


Figure 39: Omni-directional SWAN sea-state histogram from 1980-2010 at PacWave North (annual mean condition)

A.2 Annual wave rose

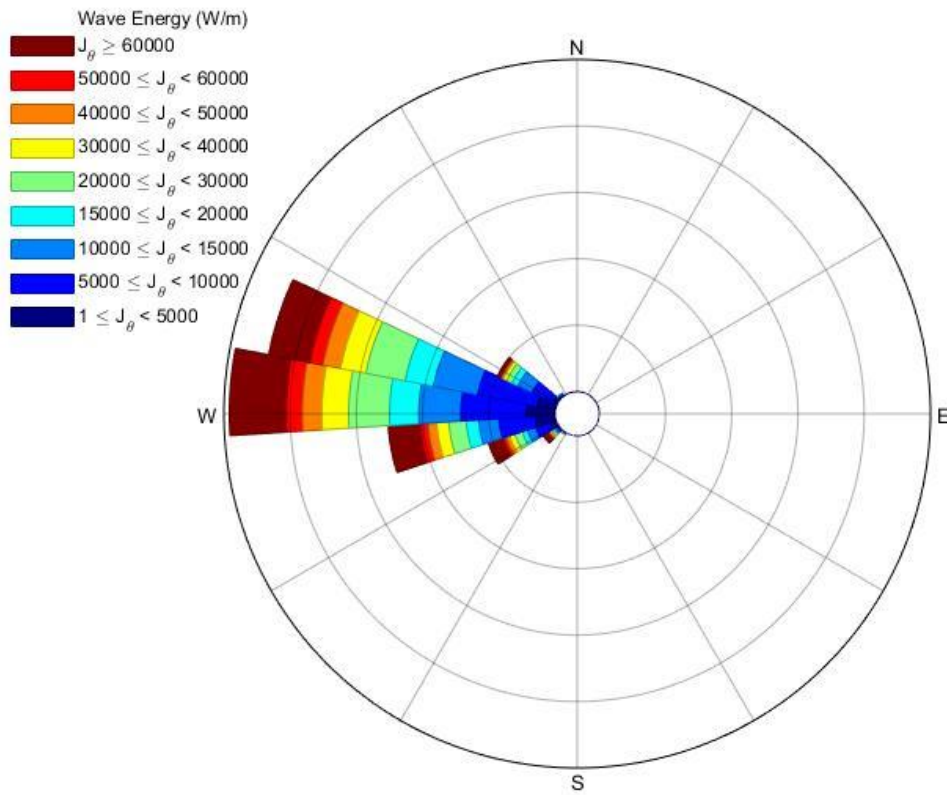


Figure 40: Directionally resolved SWAN wave rose distribution of wave energy from 1980-2010 at PacWave North

A.3 Annual variation of long-term monthly mean

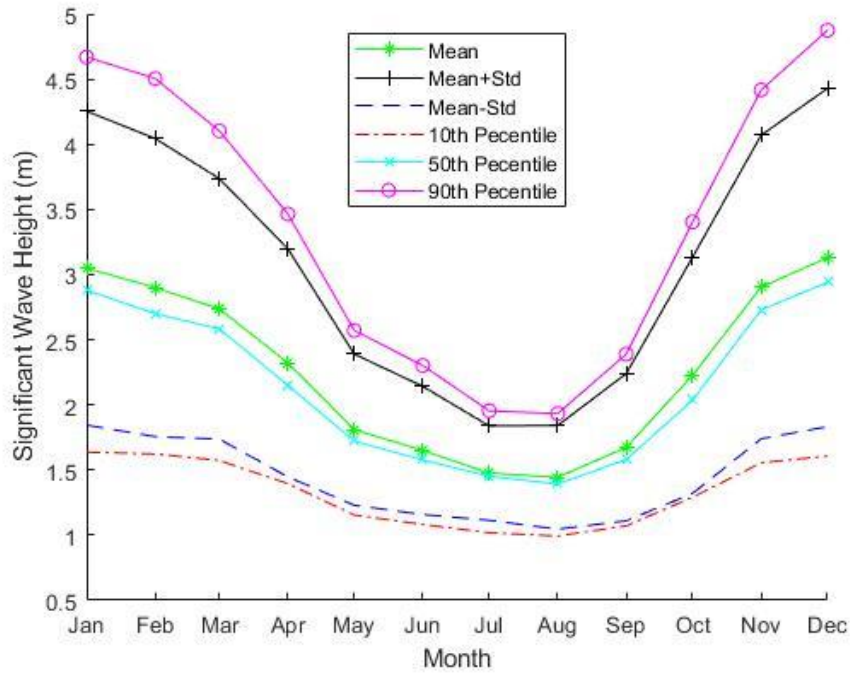


Figure 41: Monthly mean of SWAN significant wave height from 1980-2010 at PacWave North

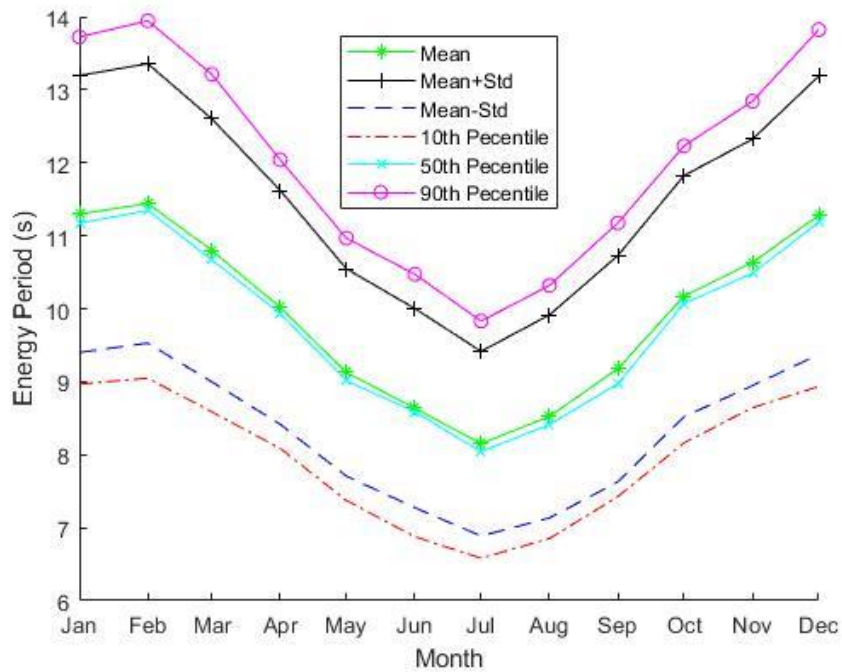


Figure 42: Monthly mean of SWAN energy period from 1980-2010 at PacWave North

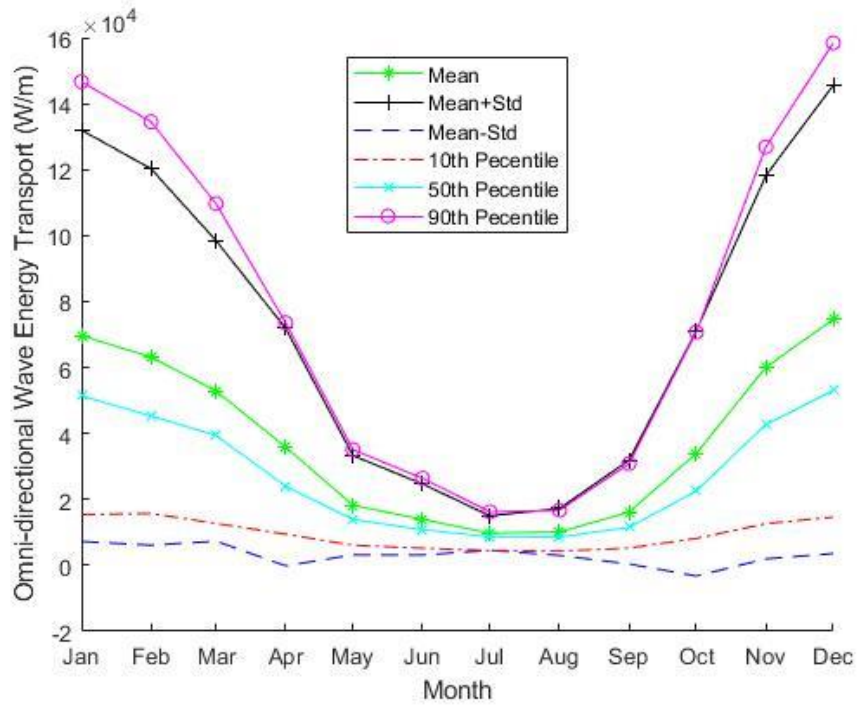


Figure 43: Monthly mean of SWAN omni-directional wave energy transport from 1980-2010 at PacWave North

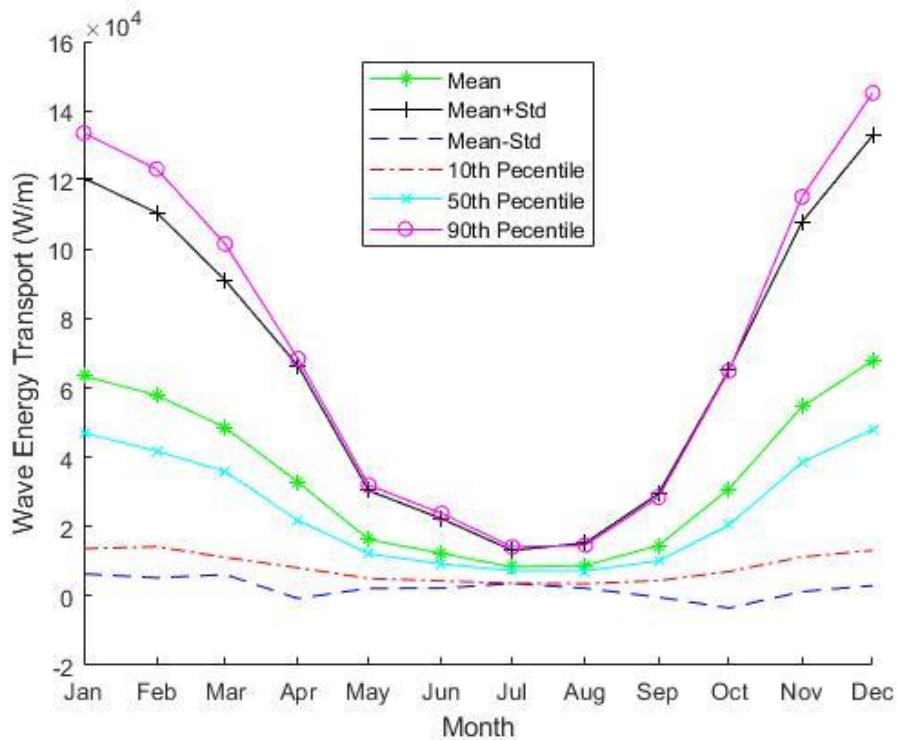


Figure 44: Monthly mean of SWAN directionally resolved wave energy transport from 1980-2010 at PacWave North

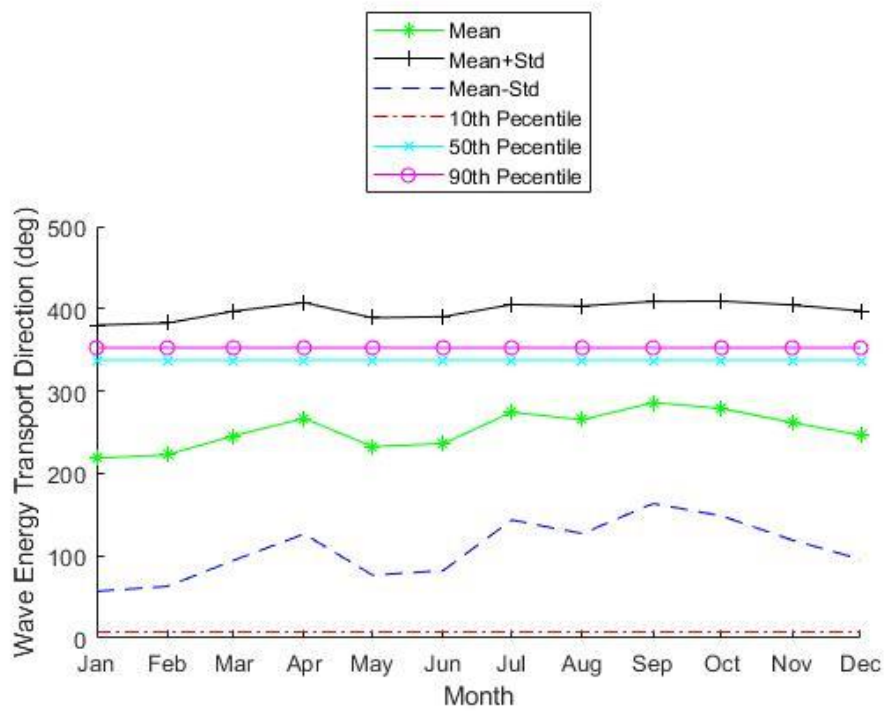


Figure 45: Monthly mean of SWAN direction of maximum directionally resolved wave energy transport from 1980-2010 at PacWave North

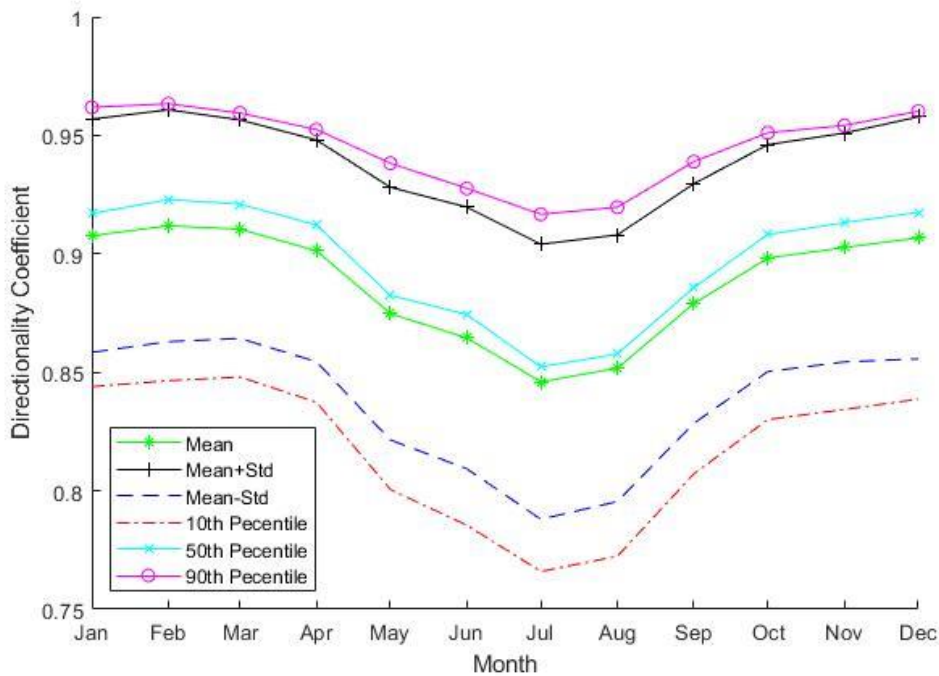


Figure 46: Monthly mean of SWAN directionality coefficient from 1980-2010 at PacWave North

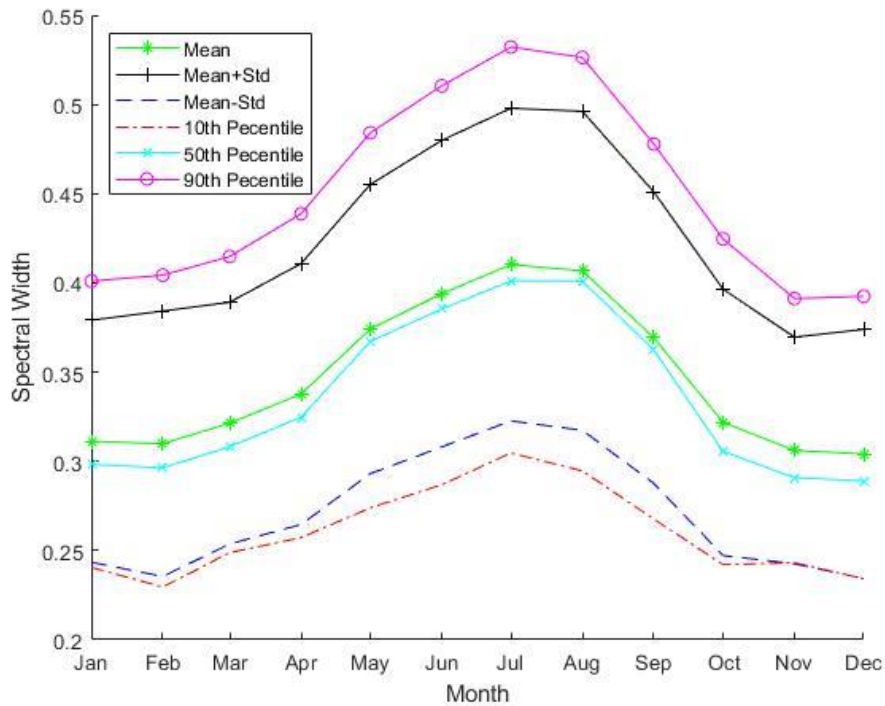


Figure 47: Monthly mean of SWAN spectral width from 1980-2010 at PacWave North

A.4 Monthly cumulative distributions

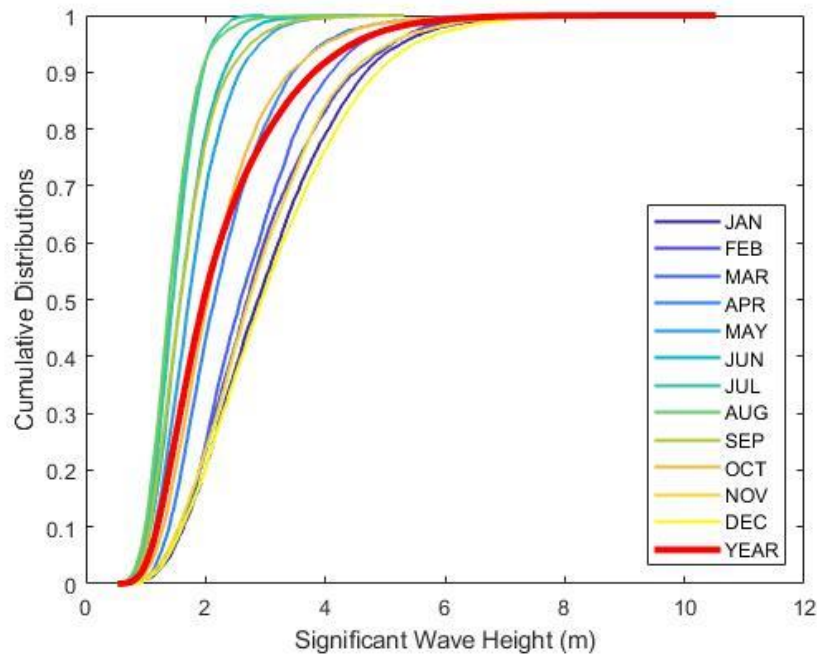


Figure 48: Monthly cumulative distributions of SWAN significant wave height from 1980-2010 at PacWave North

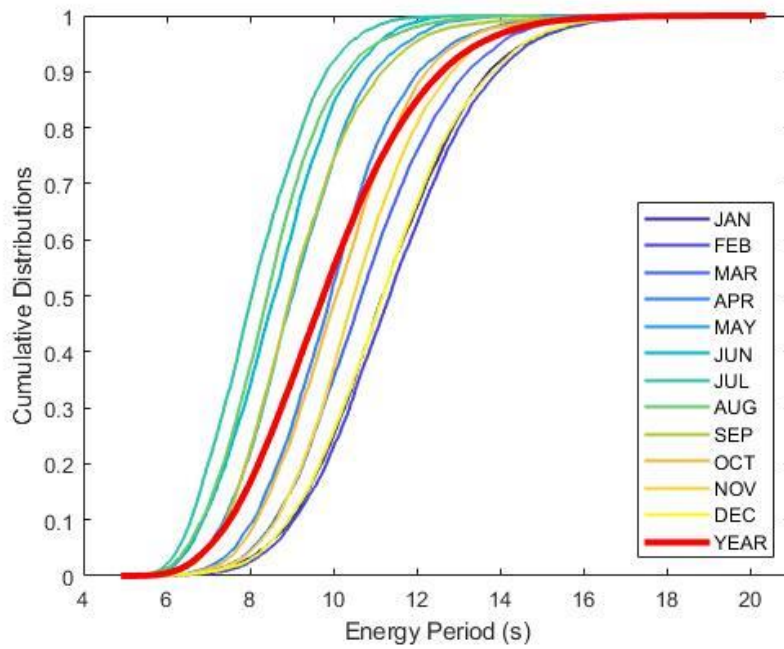


Figure 49: Monthly cumulative distributions of SWAN energy period from 1980-2010 at PacWave North

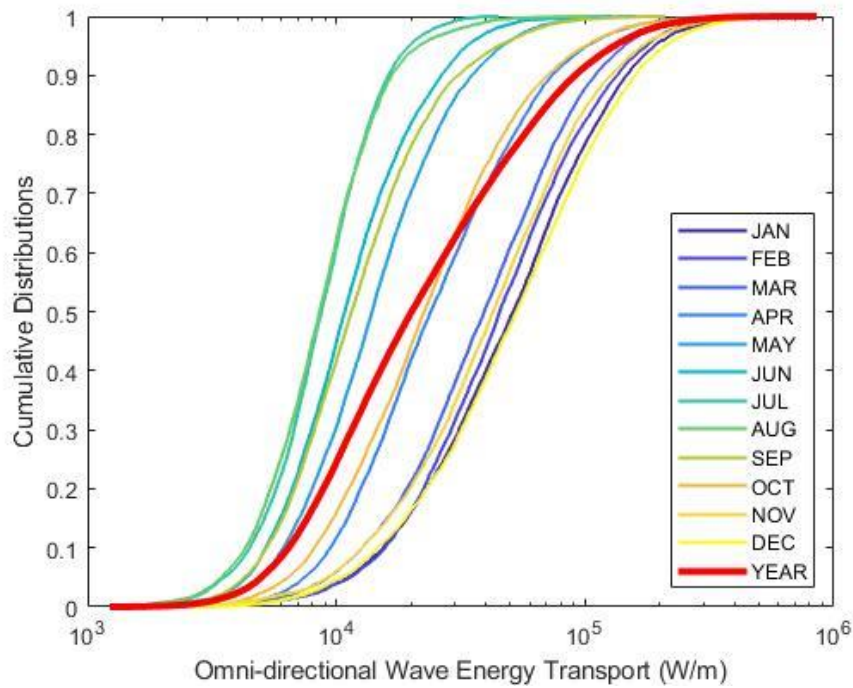


Figure 50: Monthly cumulative distributions of SWAN omni-directional wave energy plotted on a log-scale from 1980-2010 at PacWave North

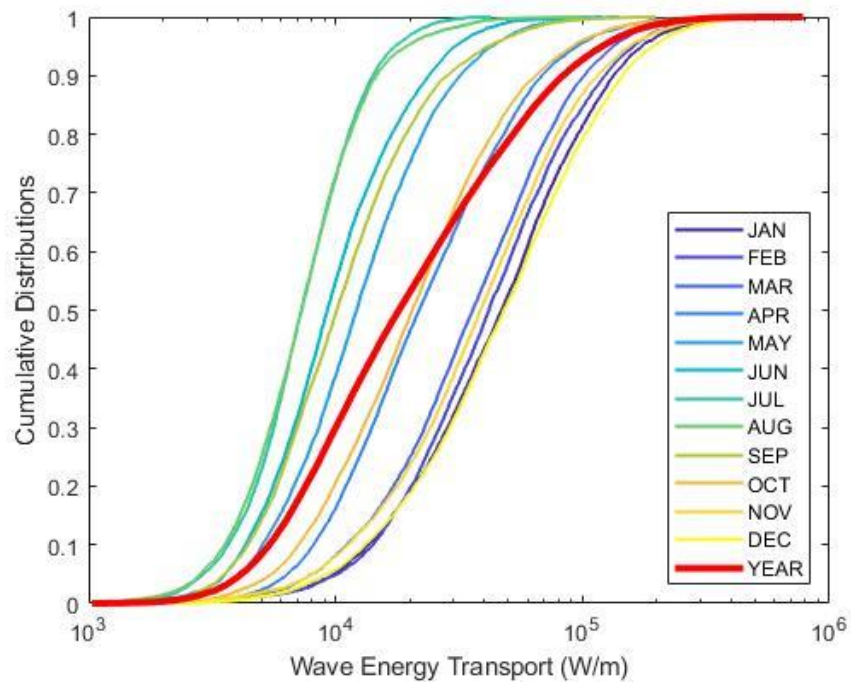


Figure 51: Monthly cumulative distributions of SWAN maximum directionally resolved wave energy transport plotted on a log-scale from 1980-2010 at PacWave North

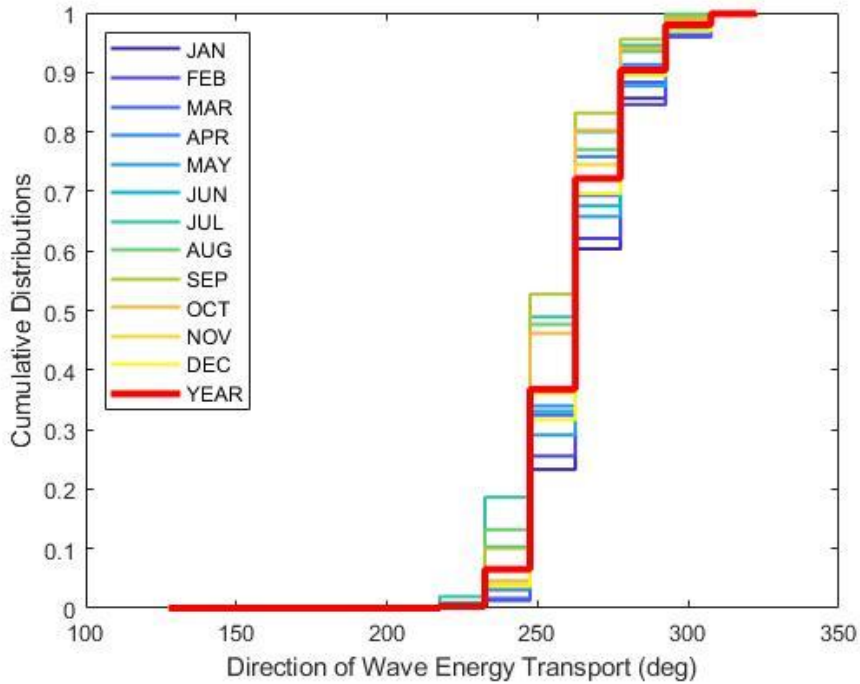


Figure 52: Monthly cumulative distributions of SWAN direction of maximum directionally resolved wave energy transport from 1980-2010 at PacWave North

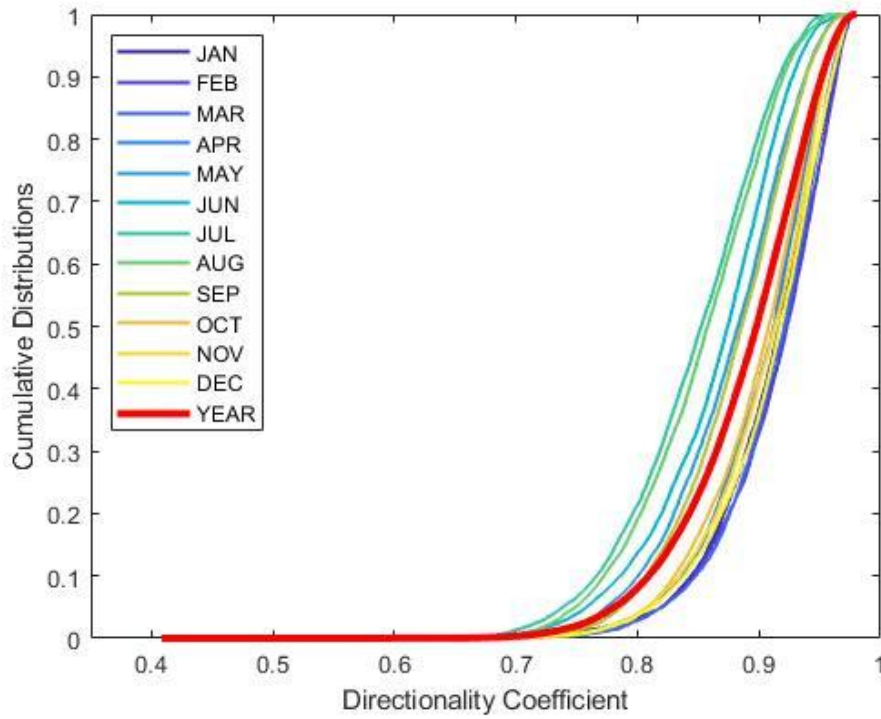


Figure 53: Monthly cumulative distributions of SWAN directionality coefficient from 1980-2010 at PacWave North

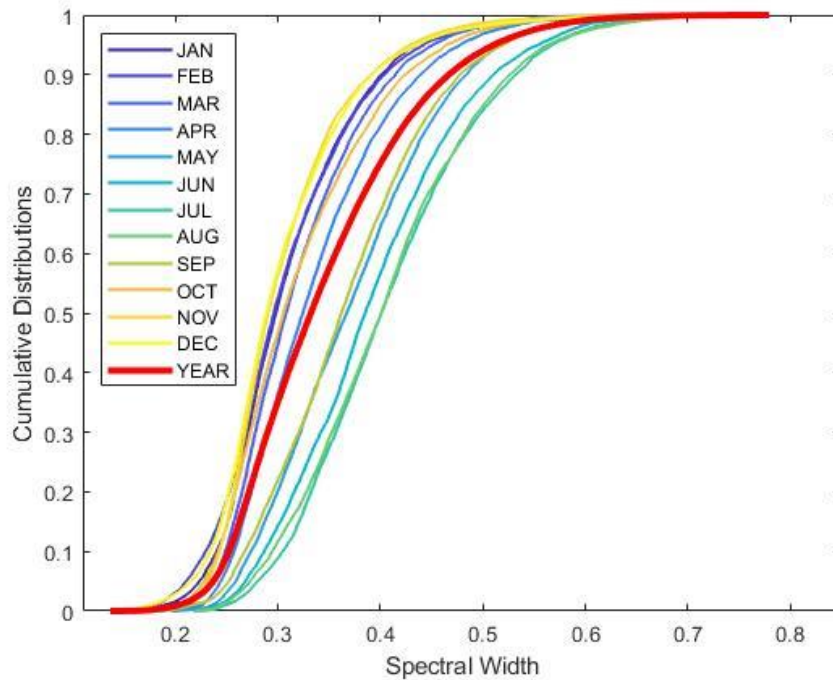


Figure 54: Monthly cumulative distributions of SWAN spectral width from 1980-2010 at PacWave North

A.6 Extreme Environmental Contours

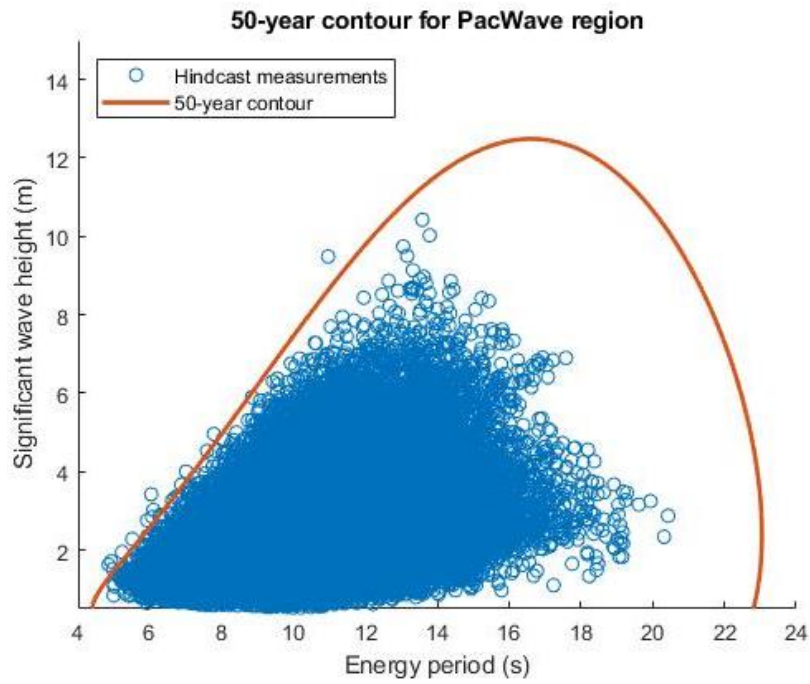


Figure 55: 50-year environmental contour for the PacWave region compared to hindcast measurements recorded for PacWave North from 1980-2010

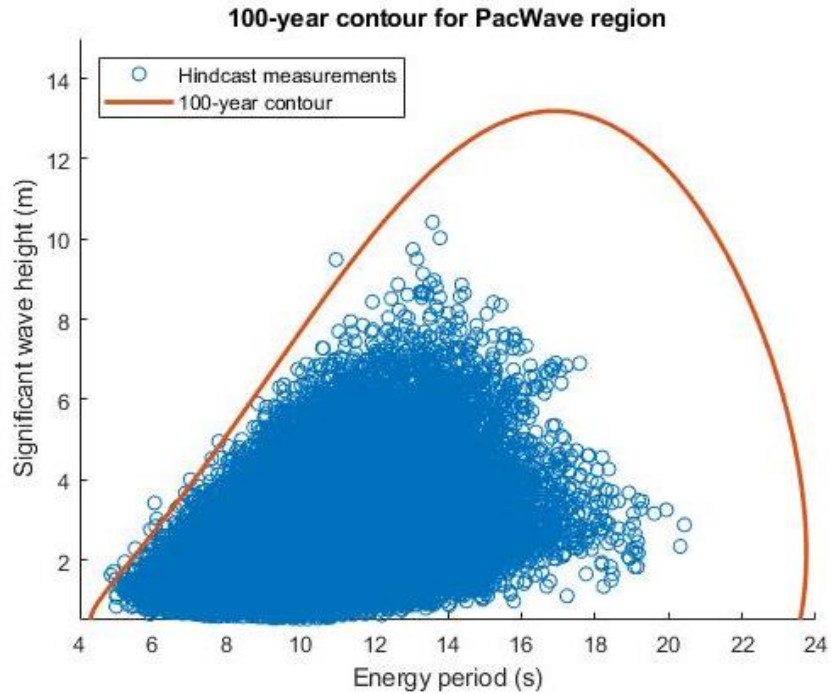


Figure 56: 100-year environmental contour for the PacWave region compared to hindcast measurements recorded for PacWave North from 1980-2010

A.7 Operation & Maintenance Windows

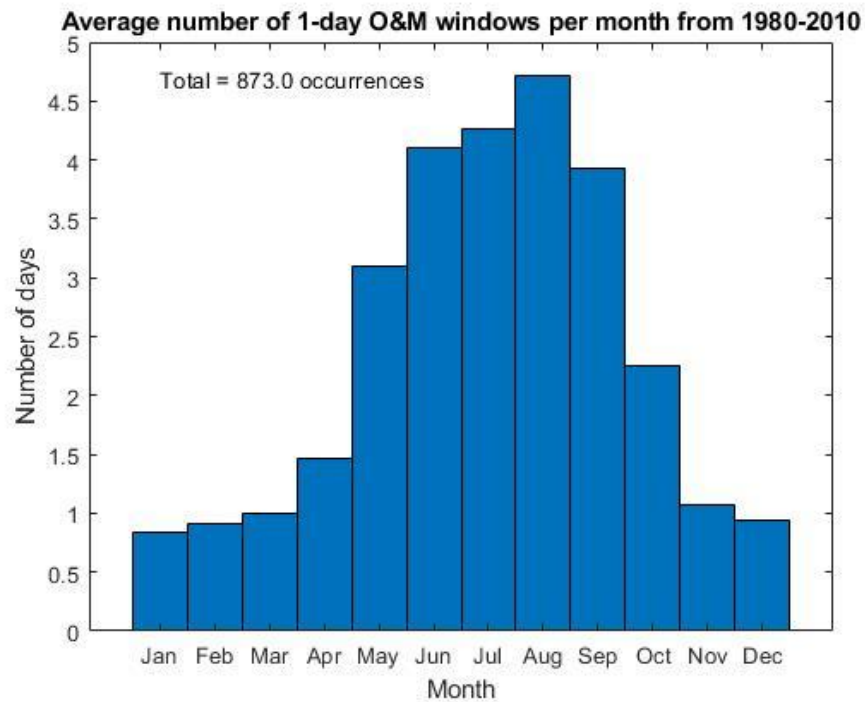


Figure 57: Number of days available for O&M from 1980-2010 at PacWave North

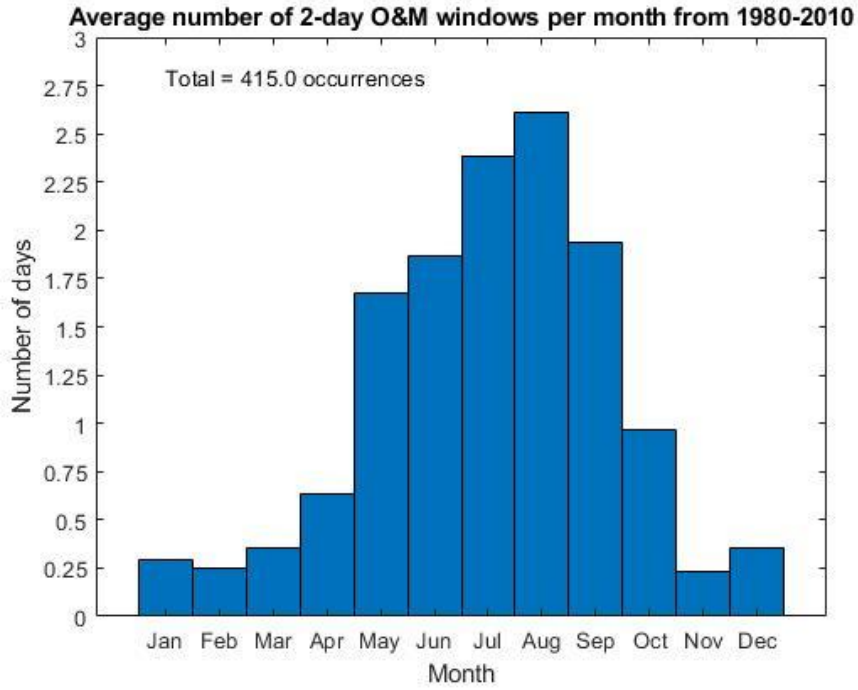


Figure 58: Number of 2-day windows for O&M from 1980-2010 at PacWave North

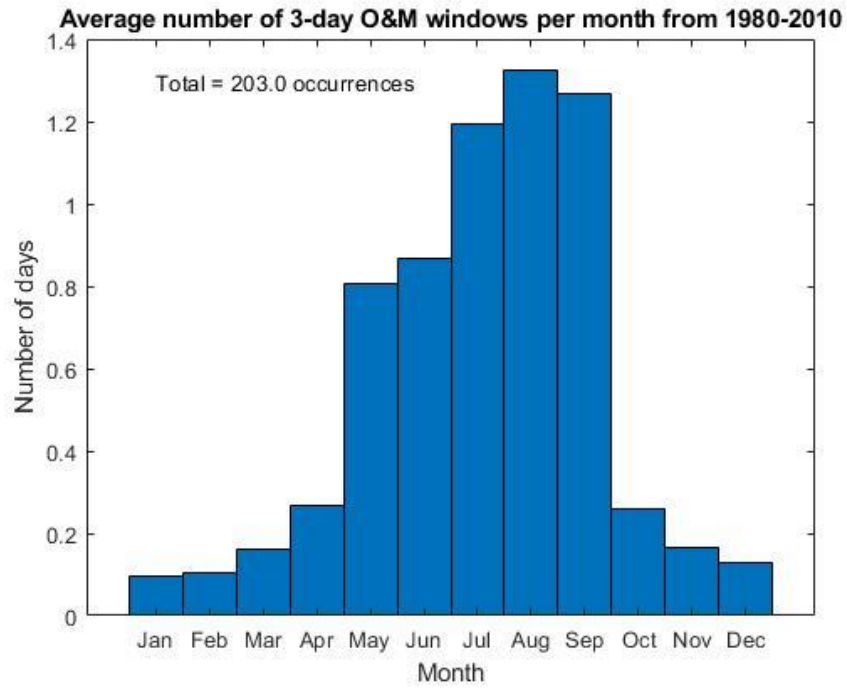


Figure 59: Number of 3-day windows for O&M from 1980-2010 at PacWave North

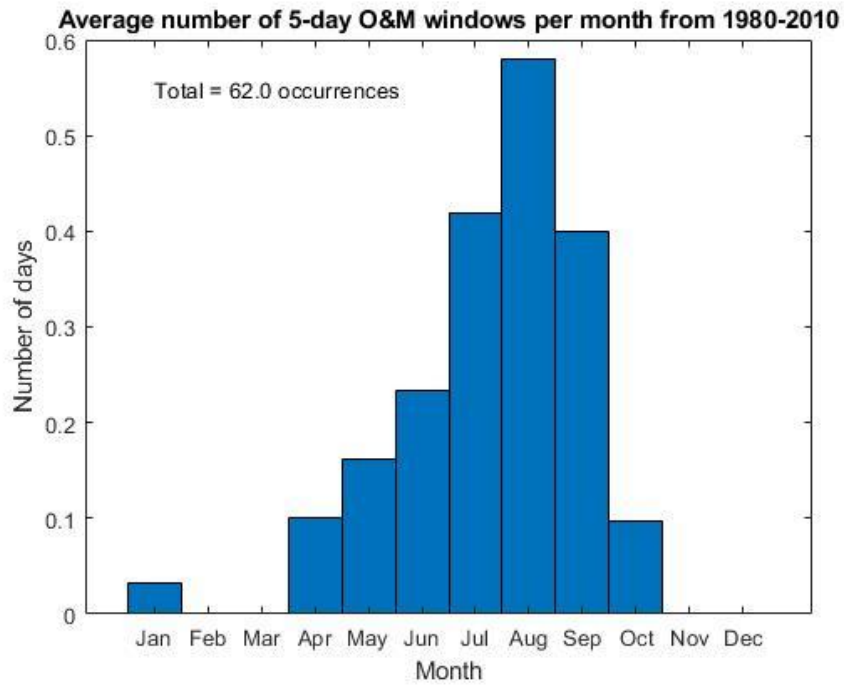


Figure 60: Number of 5-day windows for O&M from 1980-2010 at PacWave North

	Jan	Feb	Mar	Apr	May	Jun	Jul	Aug	Sep	Oct	Nov	Dec
1-day windows	0.8	0.9	1	1.5	3.1	4.0	4.3	4.7	3.8	2.2	1.0	0.9
2-day windows	0.3	0.2	0.4	0.6	1.7	1.8	2.4	2.6	1.9	1.0	0.2	0.3
3-day windows	0.1	0.1	0.2	0.3	0.8	0.9	1.2	1.3	1.3	0.3	0.2	0.1
5-day windows	0	0	0	0.1	0.2	0.2	0.4	0.6	0.4	0.1	0	0

Table 3: Average number O&M windows per month from 1980-2010 at PacWave North

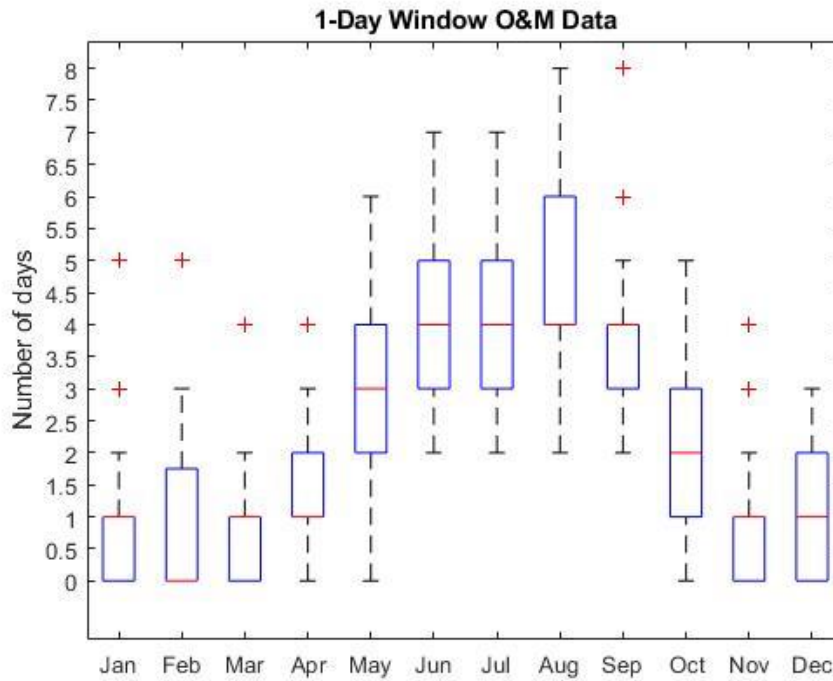


Figure 61: Box and whisker plot describing the 1-day window O&M data at PacWave North. Shown in the plot are extreme outlier values, non-extreme minima and maxima, median values (50th percentiles), and 25th and 75th percentile values.

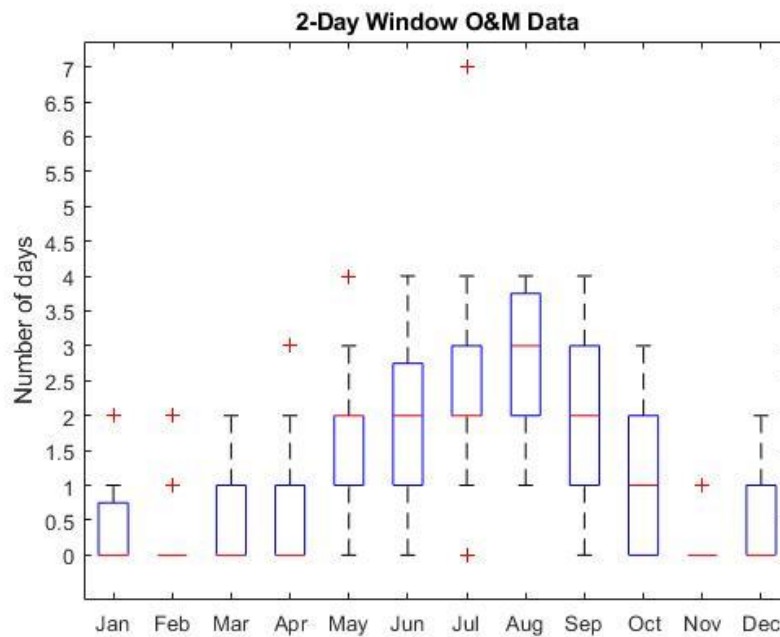


Figure 62: Box and whisker plot describing the 2-day window O&M data at PacWave North. Shown in the plot are extreme outlier values, non-extreme minima and maxima, median values (50th percentiles), and 25th and 75th percentile values.

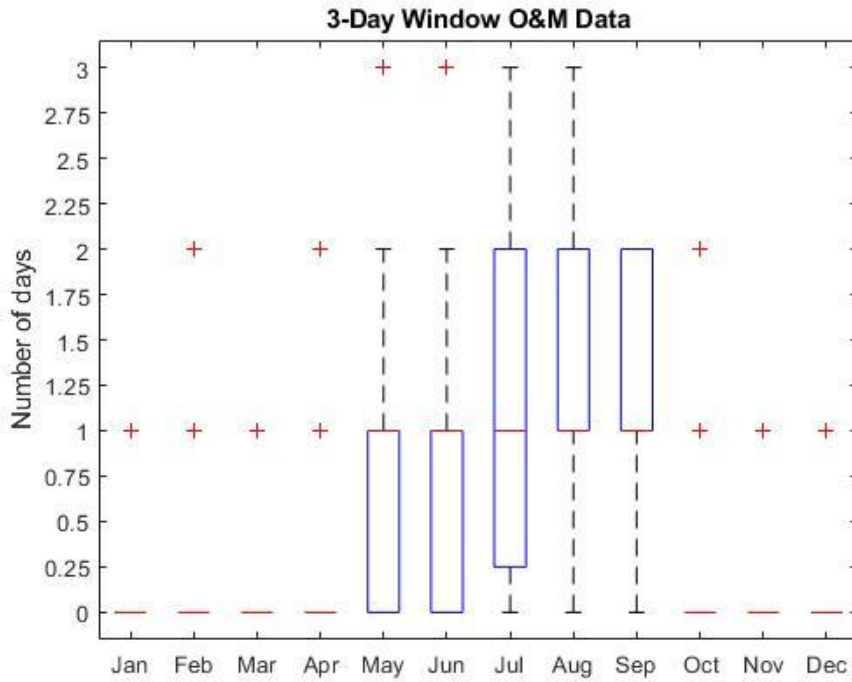


Figure 63: Box and whisker plot describing the 3-day window O&M data at PacWave North. Shown in the plot are extreme outlier values, non-extreme minima and maxima, median values (50th percentiles), and 25th and 75th percentile values.

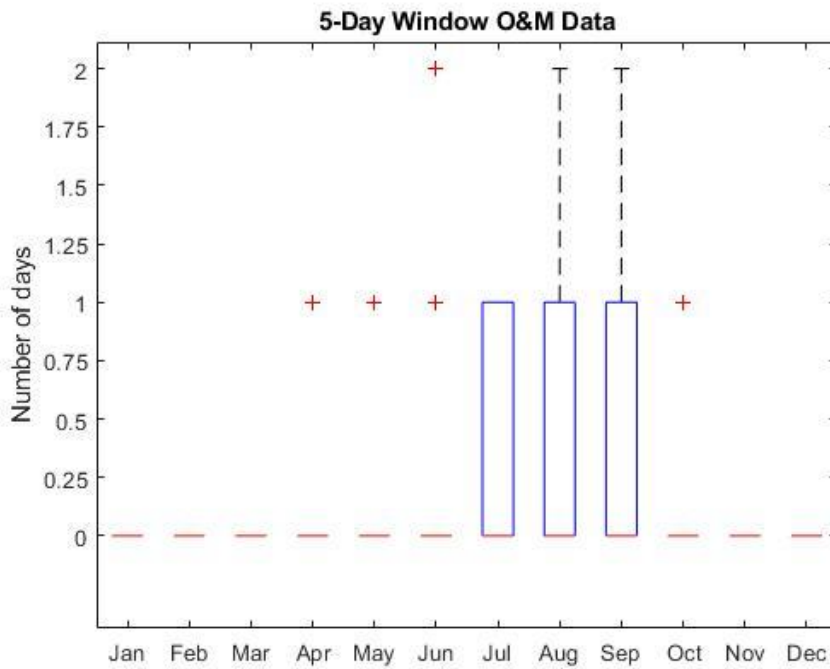


Figure 64: Box and whisker plot describing the 5-day window O&M data at PacWave North. Shown in the plot are extreme outlier values, non-extreme minima and maxima, median values (50th percentiles), and 25th and 75th percentile values.